Final Report on CRS Side Impact Study of Repeatability and Reproducibility using a Deceleration Sled

Purchase Order Number: DTNH22-15-P-00125

Report Number:

Prepared by:
Kettering University Crash Safety Center
Flint MI 48504 USA

Submitted to:
Department of Transportation
National Highway Traffic Safety Administration
Washington DC, 20590

July 2017

1. Report No.	2. Government Accession No.	3. Recipient's Catalog No.

4. Title and Subtitle	5. Report Date
Final Report on CRS Side Impact Study of Repeatability and Reproducibility using a Deceleration Sled	July 2017
	6. Performing Organization Code Kettering University Crash Safety Center
7. Author(s) Janet Brelin-Fornari, PhD, PE	8. Performing Organization Report No. DOT_SIDE_061-DOT_SIDE_ 079
9. Performing Organization Name and Address Kettering University Crash Safety Center 1700 W. University Ave. Flint, MI 48504	10. Work Unit No. (TRAIS)
	11. Contract or Grant No. DTNH22-15-P-00125
12. Sponsoring Agency Name and Address National Highway Traffic Safety Administration 1200 New Jersey Avenue, S.E. Washington, DC 20590	13. Type of Report and Period Covered Research and Development September 2015 – July 2017
	14. Sponsoring Agency Code

15. Supplementary Notes

16. Abstract

This report presents the results of the child seat side impact tests performed at Kettering University's Crash Safety Center for the National Highway Traffic Safety Administration (NHTSA). The test series was conducted using a deceleration sled. The objective of this testing was to obtain data for the analysis of repeatability within the Kettering University Crash Safety Center and reproducibility with respect to the NHTSA Vehicle Research Test Center (VRTC) testing.

Tests DOT_SIDE_061 through DOT_SIDE_079 were conducted under this contract.

17. Key Word	18. Distribution Statement
Side impact development, child restraint system, deceleration sled	

19. Security Classif. (of this report)	20. Security Classif. (of this page)	21. No. of Pages	22. Price

This final test report was prepared for the US Department of Transportation, National Highway Traffic Safety Administration, in response to Contract Number DTNH22-15-P-00125.

Prepared by: _____ Date:
Janet Brelin-Fornari, PhD, PE, Director

FINAL REPORT ACCEPTED BY:

_____

_____
Date of Acceptance

Table of Contents

Executive Summary

This report presents the results of child restraint system (CRS) side impact testing performed at Kettering University's Crash Safety Center (KCS) for the National Highway Traffic Safety Administration (NHTSA) under Purchase Order DTNH22-15-P-00125[1]. The objective of the Purchase Order was to evaluate and compare kinematic/dynamic responses in side impact sled-on-sled tests in support of NHTSA's child restraint side impact test procedure development.

Three (3) side impact baseline tests were conducted to assess the repeatability at KCS using the deceleration sled and the reproducibility of the deceleration tests with respect to the acceleration sled tests conducted at NHTSA Vehicle Research and Test Center (VRTC). Testing utilized a forward facing Graco Comfort Sport CRS and an instrumented Q3s anthropomorphic test device (ATD). The acceleration pulse fell into the corridor for all tests when testing with a secondary sled weighing 294 lb and 90 psi aluminum honeycomb (PACL-XR1-2.3-1/4-10-P-5052 from Plascore). The testing demonstrated repeatability on the deceleration sled with a 5.1% coefficient of variation (CV) for HIC15 and 4.9% CV for Chest Y Deflection. The CV for testing conducted on the acceleration sled at NHTSA/VRTC was 4.0% for HIC15 and 3.1% for Chest Y Deflection. When assessing the overall CV for both deceleration and acceleration sled testing, HIC15 and Chest Y Deflection were 4.8% and 4.5%, respectively.

With demonstrated baseline repeatability and reproducibility, an additional eighteen (18) sled-on-sled side impact tests were conducted using the development test procedure with various CRS and the CRABI 12 or Q3s ATDs in the forward and rearward facing positions. The HIC15 measures from the Q3s for each unique test combination reported less than 5% CV. The Chest Y Displacement measures from the Q3s in the forward facing orientation for each unique CRS reported less than 5% CV. The Chest Y Displacement measures from the Q3s in the rear facing orientation for each unique CRS reported a higher CV of 15% to 16%. The head-to door contact for all CRABI 12 unique test combinations of CRS and seat orientation, reported "No Contact".

Additional observations were discerned during the study:

- ✓ Head motion analysis was completed for the deceleration sled CRS specific tests to be utilized for further study in reproducibility by NHTSA/VRTC. In the forward facing CRS orientation, the results indicated the head reaches a maximum forward position and begins to rebound back toward the seatback when the secondary sled contacts the aluminum honeycomb. Therefore, both head position and direction of motion could be sources of variability.

[1] "DECEL SI Reproducibility Testing", Requisition Reference Number DTNH2215RQ-00554, September 28, 2015

- ✓ The CRABI 12 elbow joint broke on the impact side. The plastic connection tab integrity could benefit from metal fabrication
- ✓ The Q3s displayed post test damage to the structure of the hip as well as the knee joints.
- ✓ A post test inspection of the bearings and the bearing rails showed no excessive wear, binding, or degradation.
- ✓ Pull tests conducted on the secondary sled indicated different values of force needed if the anti-rebound pedal is engaged and if it has been lubricated. To remove any variability with friction on the secondary sled during run-up, it is recommended to remove the anti-rebound pedal if possible.
- ✓ The fixture seat bight width should be defined on the drawing package since an opening larger than 70 mm can affect the ability to properly install a rear facing CRS.

1.0 Objective

This report presents the results of child restraint system (CRS) side impact testing performed at Kettering University's Crash Safety Center (KCS) for the National Highway Traffic Safety Administration (NHTSA) under Purchase Order DTNH22-15-P-00125[2]. The objective of the Purchase Order was to evaluate and compare kinematic/dynamic responses in side impact sled-on-sled tests in support of NHTSA's child restraint side impact test procedure development. Under the Purchase Order, eighteen (18) sled-on-sled side impact tests were conducted using the development test procedure to further demonstrate repeatability on a decelerating sled system. The decelerating sled system was also used to demonstrate reproducibility with comparable NHTSA Vehicle Research and Test Center (VRTC) tests.

2.0 Test Plan

NHTSA was seeking to evaluate test parameters and methodologies associated with reproducing a representative side impact crash scenario on a decelerating sled system[3]. In 2013, KCS reported on previous testing[4] it had conducted under contract DTNH22-11-R-00204 to support NHTSA's Notice of Proposed Rulemaking (NPRM) (79 FR 4570, January 28, 2014; reopening of comment period, 79 FR 32211, June 4, 2014) which proposes to amend Federal Motor Vehicle Safety Standard (FMVSS) No. 213, "Child restraint systems" to adopt side impact performance requirements for child restraint systems designed for children (infants and toddlers) weighing up to 18 kilograms (40 pounds). This test series utilizes the KCS deceleration sled system to further support NHTSA's objectives.

The deceleration sled system at Kettering University was manufactured and installed by Global Testing and Engineering Services in Fraser Michigan. The sled utilizes a dual pneumatic drive to propel the test fixture down the test track at the desired test speed. At impact, the sled/test fixture strikes a tunable hydraulic decelerator causing a collision event.

The side impact test fixture being utilized consists of two distinct parts: the primary sled and the secondary sled. The primary sled is fixed to the bedplate of the deceleration sled and consists of the fixture base plate, door fixture (with foams), and aluminum honeycomb. The secondary sled consists of the generic vehicle seat (with foam and cover), the CRS being tested, and the anthropomorphic test device (ATD). The secondary sled is free to move on a set of linear bearings affixed to the primary sled base plate. The test fixture is shown in Figure 1.

[2] "DECEL SI Reproducibility Testing", Requisition Reference Number DTNH2215RQ-00554, September 28, 2015
[3] "DECEL SI Reproducibility Testing", Requisition Reference Number DTNH2215RQ-00554, September 28, 2015
[4] Brelin-Fornari, J., & Janca, S. (2014). *Development of NHTSA's Side Impact Test Procedure for Child Restraint Systems Using a Deceleration Sled: Final Report, Part 2* (No. DOT HS 811 995).

Figure 1: Side impact fixture attached to the deceleration sled

The side impact test fixture was built in support of KCS' previous work with NHTSA. In this current series of tests, NHTSA provided an updated drawing package titled "Child Side Impact Sled" dated February 2016 that slightly modified the sliding seat and wall structure. A list of additional fixture modifications is outlined in Appendix A: Fabrication of the Secondary Sled. When fabrication was complete, the final weight of the secondary sled test fixture was 294lb.

With the fixed weight of the secondary sled of 294 lb, the appropriate aluminum honeycomb pressure and size was chosen (Appendix B: Secondary Sled acceleration Pulse Development) to achieve the target deceleration corridor (Table 1) for the given test speed of 19.5 $\pm$ 0.5 mph. The aluminum honeycomb properties and size utilized were:

- ✓ Plascore aluminum honeycomb PACL-XR1-2.3-1/4-10-P-5052, 90 PSI ± 5%
- ✓ Aluminum honeycomb test size of 305 mm (depth) by 343 mm by 108 mm (12" x 13.5" x 4.25") with a total of 928 complete (active) cells (Figure 2)

Table 1: Secondary sled acceleration corridor

Upper		Lower	
Time (ms)	Acceleration (g)	Time (ms)	Acceleration (g)
0	0.5	2	0
6	25.5	13	18.5
44	25.5	40	18.5
58	0	48	0

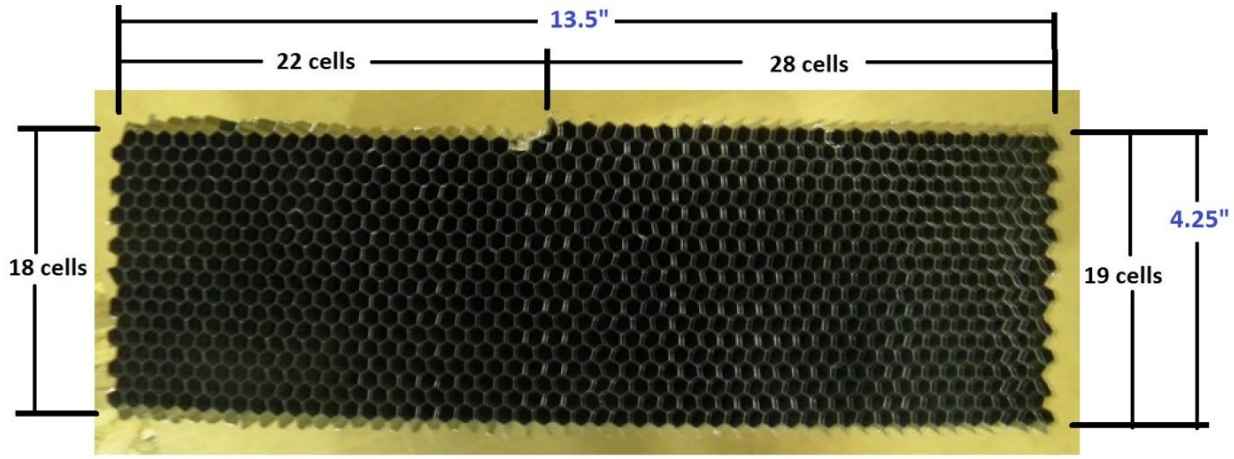

Figure 2: Aluminum honeycomb with 928 complete (active) cells

The tests were conducted in both forward and rear facing orientation. The Q3 side (Q3s) three-year-old and the Child Restraint/Air Bag Interaction twelve-month-old (CRABI 12) ATDs were utilized. The ATD instrumentation is listed in Table 2. A complete guide for KCS testing setups, procedures, and documentation is listed in Appendix C: Deceleration Sled Side Impact Test Procedure.

Table 2: ATD instrumentation

Instrumentation Channel	**Q3s (number of channels)**	**CRABI 12 (number of channels)**
Head cg triax accelerometer	3	3
Neck upper load cell Forces Fy, Fz Moment Mx	3	3
Shoulder displacement Y	1	n/a
Chest triaxial accelerometer	n/a	3
IR-TRACC Displacement	1	n/a
Spine Y-axis accelerometer	1	n/a
Pelvis Y-axis accelerometer	1	1
Total	**10**	**10**

Five (5) accelerometers were attached to the side impact fixture. Two (2) accelerometers were utilized on the main deceleration sled (primary and redundant). Three (3) distinct accelerometers were utilized on the secondary sled (Table 3). The three (3) secondary sled accelerometers were attached to the right rear leg structure at the vertical positions depicted in Figure 3. Since it was determined that accelerometer positioning can affect the measured acceleration value (Appendix B: Secondary Sled acceleration Pulse Development), the same model accelerometers were placed in the same structural positions as the NHTSA/VRTC acceleration sled tests.

Table 3: Accelerometers utilized on the secondary sled

Accelerometer	Damped or Undamped	Position from bottom of box tube frame
Endevco 7290 E	Damped	190 mm (Upper)
Endevco 7231 C	Undamped	155 mm (Mid)
Endevco 7231 C	Undamped	110 mm (Lower)

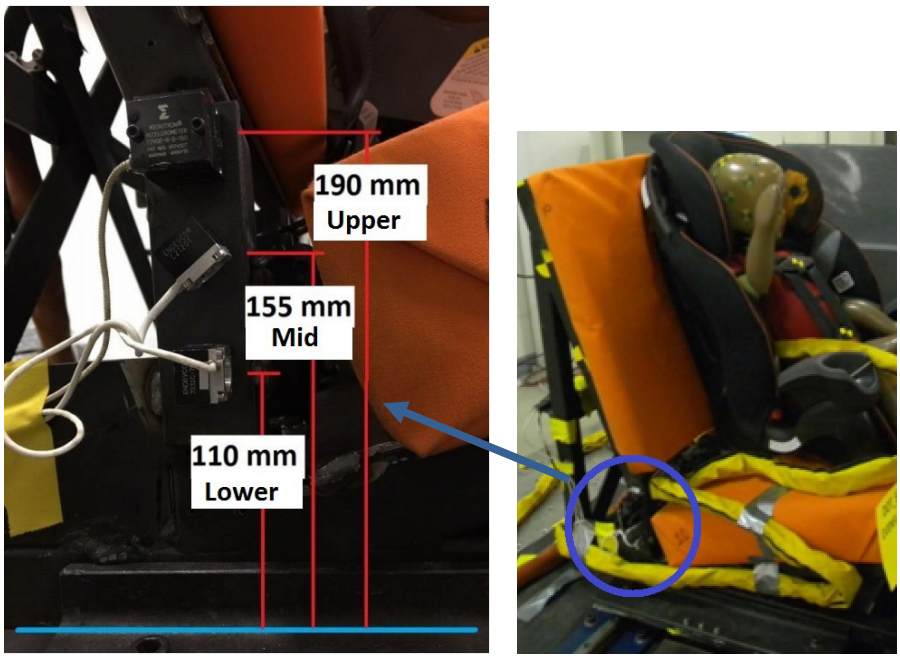

Figure 3: Accelerometer locations - dimensions measured from the bottom of the sled rail

3.0 Baseline Repeatability and Reproducibility

Three (3) tests, DOT_SIDE_050, 051, and 052, were conducted as a Baseline to assess KCS deceleration sled repeatability and KCS deceleration sled reproducibility with respect to NHTSA/VRTC acceleration sled testing. The tests utilized a forward facing Graco Comfort Sport CRS with an instrumented Q3s in the forward facing orientation. Data was collected and analyzed with respect to secondary sled acceleration time history and impact speed as well as ATD HIC15 and chest displacement.

The accelerations measured on the secondary sled in each of the three accelerometer positions, fell within the corridor and were comparable to the accelerations measured at NHTSA/VRTC (Figure 4 through 6).

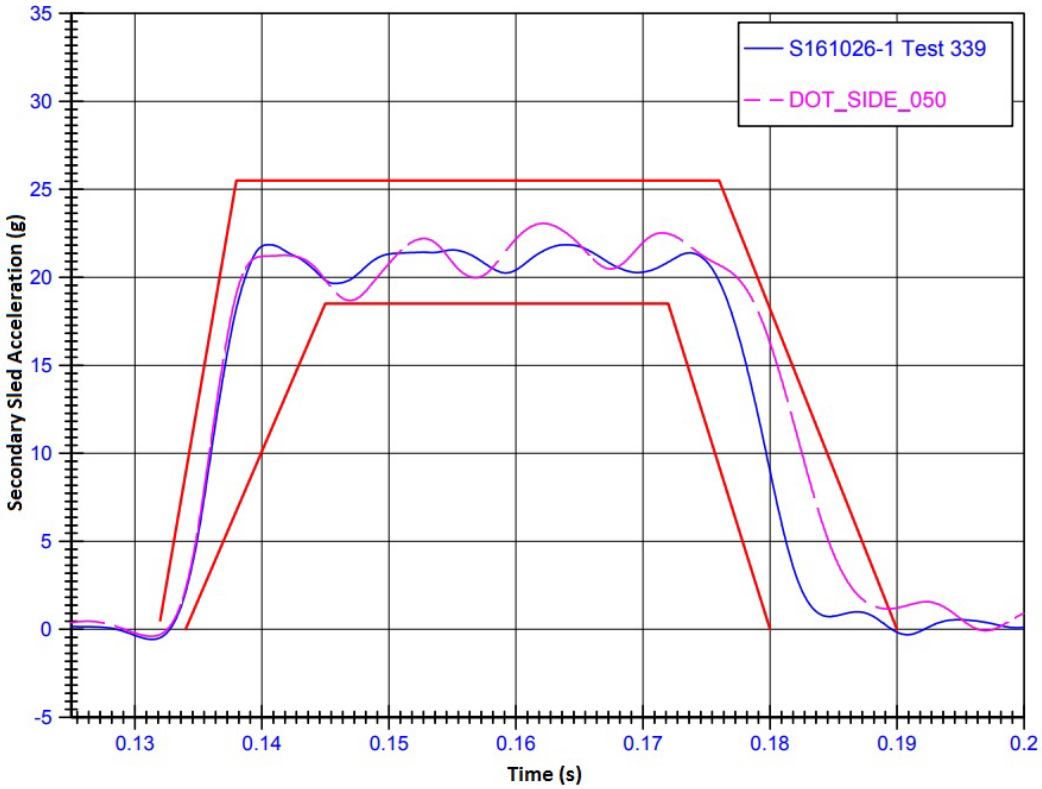

Figure 4: Upper acceleration measurement with corridor

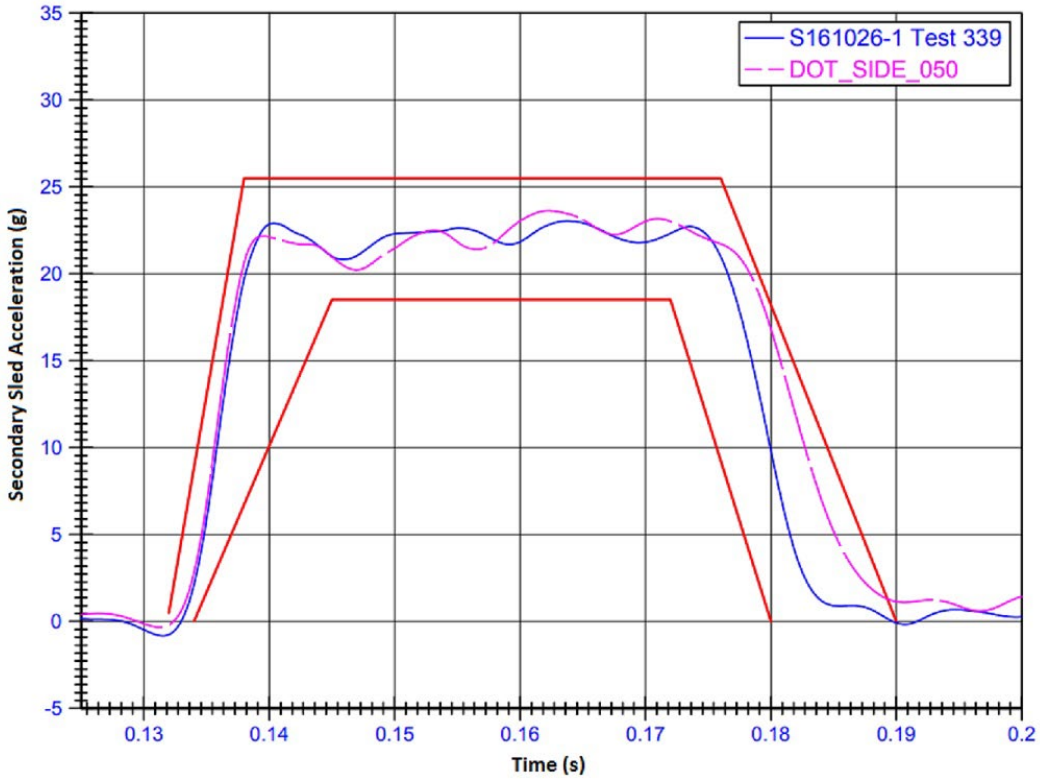

Figure 5: Mid acceleration measurement with corridor

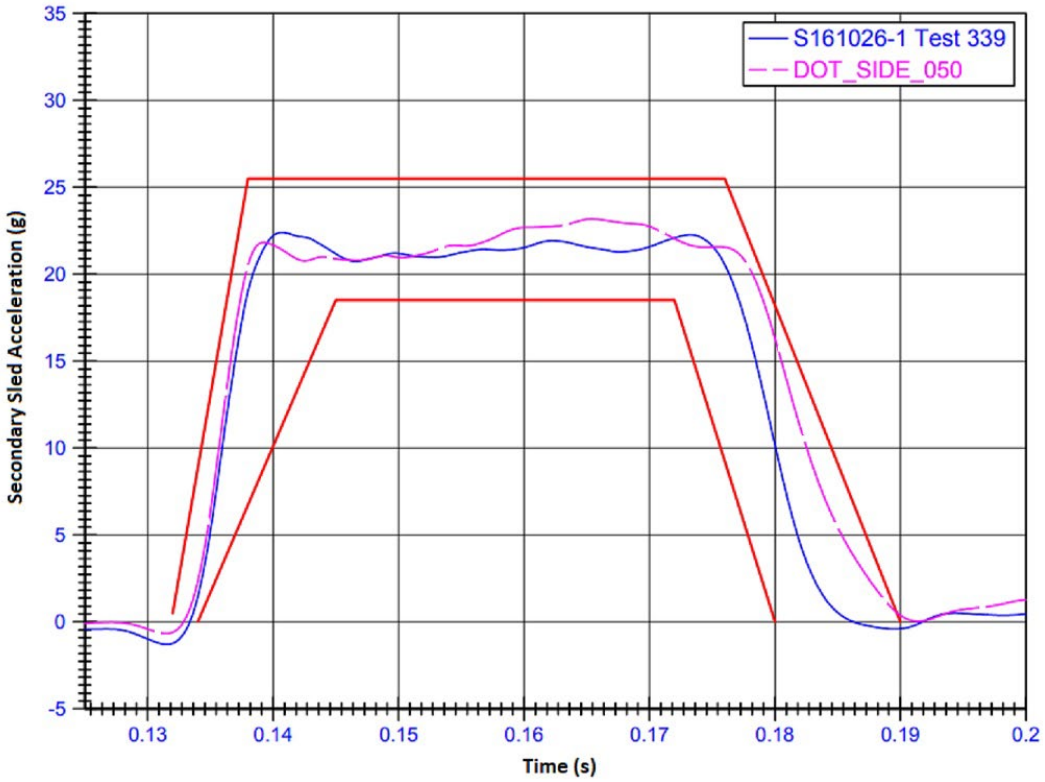

Figure 6: Lower acceleration measurement with corridor

All tests met the critical parameter of impact speed as measured by at least two of the three accelerometers (Table 4) and calculated per the relative velocity calculation process defined in Appendix D: Calculation of Relative Velocity.

Table 4: Relative velocity as measured by the Upper, Mid, and Lower accelerometers for KCS and NHTSA/VRTC testing

Test	Relative Velocity - Upper (7290E) (mph)	Relative Velocity - Mid (7231C) (mph)	Relative Velocity - Lower (7231C) (mph)
Kettering 050	19.68	19.51	20.12
Kettering 051	19.31	19.38	19.75
Kettering 052	19.48	19.52	19.86
VRTC 339	19.69	19.51	19.66
VRTC 340	19.74	19.53	19.59
VRTC 345	19.72	19.49	19.60

The HIC15 and Chest Y Displacement were compared within each facility and overall. The coefficient of variation (CV), as defined by the standard deviation divided by the mean, was calculated for each group (Tables 5 and 6). The overall coefficient of variation was less than 5%.

Table 5: Coefficient of variation for HIC15 for the KCS tests, NHTSA/VRTC tests, and overall

Test	HIC15	CV
Kettering 050	766	5.1%
Kettering 051	695	
Kettering 052	751	
VRTC 339	672	4.0%
VRTC 340	716	
VRTC 345	724	
Overall Coefficient of Variation (CV)		4.8%

Table 6: Coefficient of variation for Chest Y Displacement for the KCS tests, NHTSA/VRTC tests, and the overall

Test	Chest Displacement (mm)	CV
Kettering 050	21.57	4.9%
Kettering 051	23.59	
Kettering 052	21.86	
VRTC 339	21.62	3.1%
VRTC 340	20.58	
VRTC 345	21.83	
Overall Coefficient of Variation (CV)		4.5%

4.0 CRS Specific Test Series

With reproducibility confirmed, the test series continued with a test matrix of eighteen (18) CRS specific tests (Table 7). Again, the KCS testing setups and procedures including fixture instrumentation, ATD instrumentation, and camera positioning are listed in Appendix C:

Deceleration Sled Side Impact Test Procedure. Results for the CRS specific tests are reported in the individual test reports DOT_SIDE_061, DOT_SIDE_062, and DOT_SIDE_064 through DOT_SIDE_079. Tabular data is listed in Appendix E: Tabular Data for Tests DOT_SIDE_061 through DOT_SIDE_079.

Table 7: Test Matrix

Test Number	Dummy Type	CRS	Orientation	Restraint
DOT_SIDE_061	Q3s	Evenflo Maestro	FF Combination	LATCH
DOT_SIDE_062	Q3s	Evenflo Maestro	FF Combination	LATCH
DOT_SIDE_067	Q3s	Evenflo Maestro	FF Combination	LATCH
DOT_SIDE_064	Q3s	Graco Comfort Sport	FF Convertible	LATCH
DOT_SIDE_065	Q3s	Graco Comfort Sport	FF Convertible	LATCH
DOT_SIDE_066	Q3s	Graco Comfort Sport	FF Convertible	LATCH
DOT_SIDE_068	Q3s	Graco Comfort Sport	RF Convertible	LA Only
DOT_SIDE_069	Q3s	Graco Comfort Sport	RF Convertible	LA Only
DOT_SIDE_070	Q3s	Graco Comfort Sport	RF Convertible	LA Only
DOT_SIDE_071	12 MTH CRABI	Chicco KeyFit 30	RF Infant	LA Only
DOT_SIDE_072	12 MTH CRABI	Chicco KeyFit 30	RF Infant	LA Only
DOT_SIDE_073	12 MTH CRABI	Chicco KeyFit 30	RF Infant	LA Only
DOT_SIDE_074	12 MTH CRABI	Britax Boulevard	RF Convertible	LA Only
DOT_SIDE_075	12 MTH CRABI	Britax Boulevard	RF Convertible	LA Only
DOT_SIDE_076	12 MTH CRABI	Britax Boulevard	RF Convertible	LA Only
DOT_SIDE_077	12 MTH CRABI	Cosco Apt 40RF	FF Convertible	LATCH
DOT_SIDE_078	Q3s	Diono Olympia	RF Convertible	LA Only
DOT_SIDE_079	Q3s	Diono Olympia	RF Convertible	LA Only

4.1 Accelerometer Position Comparison

The acceleration pulse as measured by the three accelerometers on the secondary sled fell within the prescribed corridor for at least two of the three measured positions as reported in the individual test reports (DOT_SIDE_061, DOT_SIDE_062, and DOT_SIDE_064 through DOT_SIDE_079)[5].

All tests met the critical parameter of impact speed (as measured by at least one accelerometer, Table 8) as calculated per the relative velocity calculation process defined in Appendix D: Relative Velocity Calculation. One additional test was conducted where the relative velocity, as measured by all three accelerometers on the secondary sled, was outside the test range of 19.5 $\pm$ 0.5 mph. It is listed in Table 8 as Test 063X. It should be noted that the speed of the secondary sled is determined at impact with the aluminum honeycomb. The point-in-time is defined by a trigger switch between the aluminum honeycomb impact plate and the aluminum honeycomb. For a CRS that is considered "wide", such as the Cosco Apt 40RF (DOT_SIDE_077) in this series, the CRS may strike the primary sled door before the impact switch is triggered.

In the deceleration sled test, the complete fixture, primary and the secondary sled, is driven to impact with the main decelerator at synchronous speed. The primary sled impacts the decelerator and decelerates while the secondary sled continues moving along the linear bearing rails for 800 mm prior to impact with the aluminum honeycomb and the door fixture. During the time when the secondary sled is moving relative to the primary sled, friction from the linear bearings and anti-rebound pedal are the only deceleration mechanisms on the secondary sled. Therefore, in order for the secondary sled to impact the honeycomb and door fixture within the prescribed speed corridor, the primary sled must be faster than the secondary sled to honeycomb impact speed. A comparison of the primary sled speed versus the secondary sled speed for the overall and each individual secondary sled accelerometer location is depicted in Figures 7 through 10.[6]

[5] DOT_SIDE_063 does not have a reported individual test report since the velocity measured by all three accelerometer locations was greater than the target test speed range of 19.5 $\pm$ 0.5 mph

[6] To conduct the testing with consistent deceleration sled input pressure (and therefore consistent primary sled overall velocity), ballast weight was added to the primary sled when the CRABI12 was utilized instead of the Q3s.

Table 8: Primary sled speed and relative velocity for the secondary sled

Test Number	Sled Overall Velocity [mph]	Relative Velocity (Upper Ax) (7290E) [mph]	Relative Velocity (Mid Ax) (7231C) [mph]	Relative Velocity (Lower Ax) (7231C) [mph]	Relative Velocity Delta Max –Min [mph]
061	20.79	19.49	19.68	19.82	0.33
062	20.74	19.57	19.74	19.92	0.35
067	20.32	19.40	19.58	19.72	0.32
064	20.72	19.66	19.84	19.91	0.25
065	20.49	19.61	19.73	19.93	0.32
066	20.38	19.52	19.75	20.10	0.58
067	20.32	19.40	19.58	19.72	0.32
068	20.34	19.44	19.75	19.84	0.4
069	20.05	19.09	19.25	19.53	0.44
070	20.04	19.11	19.40	19.56	0.45
071	20.29	19.43	19.65	19.91	0.48
072	20.17	19.29	19.46	19.68	0.39
073	20.06	19.10	19.30	19.59	0.49
074	20.08	19.09	19.33	19.64	0.55
075	20.06	19.12	19.27	19.65	0.53
076	20.12	18.99	19.14	19.41	0.42
077	20.06	18.92	19.14	19.48	0.56
078	20.18	19.08	19.44	19.87	0.79
079	19.92	18.45	18.81	19.36	0.91
063X	21.37	20.27	20.46	20.65	0.38

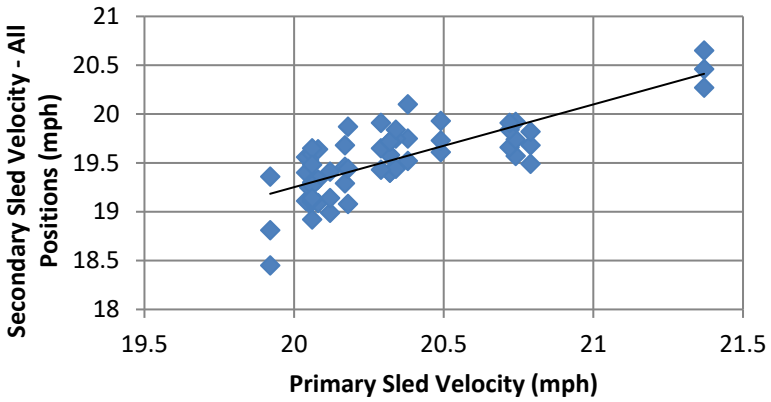

Figure 7: Secondary sled velocity (all positions) versus primary sled velocity

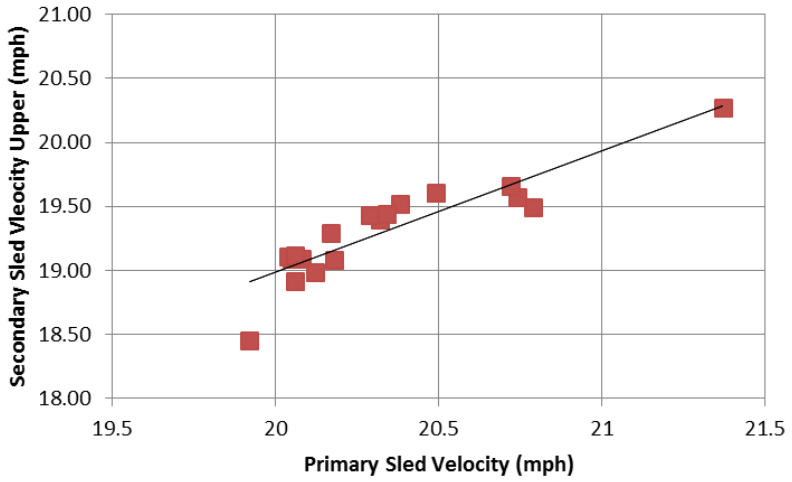

Figure 8: Secondary sled velocity (Upper Ax) versus primary sled velocity

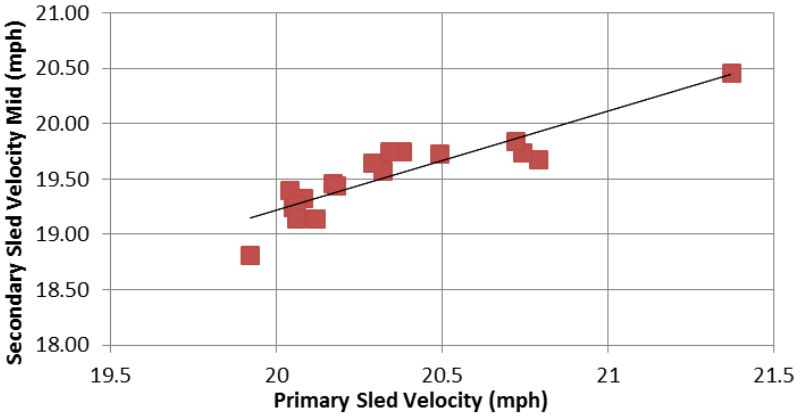

Figure 9: Secondary sled velocity (Mid Ax) versus primary sled velocity

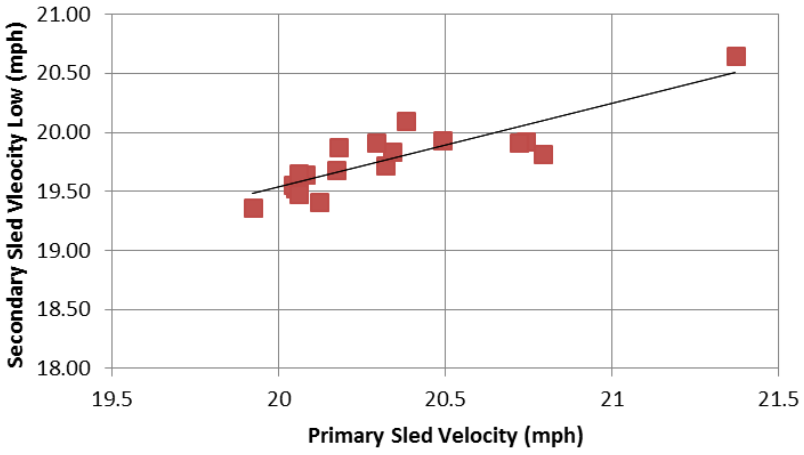

Figure 10: Secondary sled velocity (Lower Ax) versus primary sled velocity

Utilizing a linear regression for the data, a secondary sled impact-to-door speed can be predicted given an incoming primary sled speed (Table 9). Note that the relationship between the primary sled speed and the secondary sled impact speed are different for the overall and individual accelerometer positions. By assessing the R^2 value, it is also noted that the individual positions have a better regression fit than the overall relationship. Therefore, for the same primary sled speed, each accelerometer will predict a different impact velocity. For example, per the regression equations, if the primary sled speed is 20.5 mph, it can be predicted that the upper accelerometer would measure 19.46 mph, mid 19.66 mph, and lower 19.89 mph. Therefore, with a 0.43 mph predicted difference in the speeds for the same primary sled speed, defining the position of the accelerometer on the secondary sled structure could improve reproducibility.

Table 9: Linear regression relationships for each accelerometer location

Acceleration Location	Linear Relationship	R^2 Value	Predicted Secondary Sled Impact Speed (mph) for a 20.5 mph Primary Sled Speed
All	y = 0.847 x + 2.311	0.590	19.67
Upper	y = 0.947 x + 0.048	0.816	19.46
Mid	y = 0.889 x + 1.438	0.819	19.66
Lower	y = 0.705 x + 5.436	0.755	19.89

4.2 ATD Metrics Analysis

Repeatability with respect to the Q3s ATD kinematics was assessed utilizing the HIC15 and Chest Y Displacement measured values (Table 10). There was less than 5% coefficient of variation in the HIC15 results per CRS for both forward facing and rear facing Q3s tests. There was less than 5% coefficient of variation in the chest deflection results per CRS for the forward facing Q3s tests. For the rear facing Q3s tests, there was a 16% coefficient of variation for the rear facing Graco Comfort Sport (Tests 68, 69, and 70) and a 15.8% coefficient of variation for the Diono Olympia (Tests 78 and 79). In both cases, the value of the greatest Chest Y Displacement correlates with the value of the greatest relative velocity.

Repeatability with respect to the CRABI 12 ATD kinematics was assessed utilizing the head-to-door impact measure as determined by the switch connection between the copper mesh on the ATD head and the metal tape on the door fixture. For all tests utilizing the CRABI 12, Head-to-Door contact did not occur (Table 11).

Table 10: Q3s HIC 15 and Chest Displacement with CRS specific Coefficient of Variations

Test Number	CRS and Orientation (FF or RF)	HIC15	HIC15 CV	Chest Dis-placement (mm)	Chest Dis-placement CV	Relative Velocity – Low Position (mph)
061	Evenflo Maestro - FF	917	4.4%	23.3	1.5%	19.82
062	Evenflo Maestro - FF	963		23.3		19.92
067	Evenflo Maestro - FF	882		23.9		19.72
064	Graco Comfort Sport - FF	693	2.1%	22.7	1.8%	19.91
065	Graco Comfort Sport - FF	665		22		19.93
066	Graco Comfort Sport - FF	683		22.7		20.10
068	Graco Comfort Sport - RF	457	3.1%	33.5	16.0%	19.84
069	Graco Comfort Sport - RF	481		26.7		19.53
070	Graco Comfort Sport - RF	483		24.9		19.56
078	Diono Olympia - RF	979	1.8%	34.3	15.8%	19.87
079	Diono Olympia - RF	955		27.4		19.36

Table 11: CRABI 12 Head-to Door contact

Test Number	CRS	Head-to-Door Contact? (Yes/No)
DOT_SIDE_071	Chicco KeyFit 30 - RF	No
DOT_SIDE_072	Chicco KeyFit 30 - RF	No
DOT_SIDE_073	Chicco KeyFit 30 - RF	No
DOT_SIDE_074	Britax Boulevard - RF	No
DOT_SIDE_075	Britax Boulevard - RF	No
DOT_SIDE_076	Britax Boulevard - RF	No
DOT_SIDE_077	Cosco Apt 40RF - FF	No

4.3 Head Motion Analysis

During deceleration sled testing with the side impact fixture, when the primary sled impacts the decelerator, the secondary sled moves along the linear bearings at a 10 degree angle with respect to the primary sled for 800 mm before impact with the aluminum honeycomb (Figure 11). During this run-up, in a forward facing orientation of the CRS, the head of the ATD nods forward (flexion) due to the acceleration field caused by the 10 degree angle. For the eighteen (18) CRS specific tests, the head displacement was tracked using TEMA motion analysis software. The head motion analysis results for all CRS specific tests in the series are located in Appendix F: Head Motion Analysis.

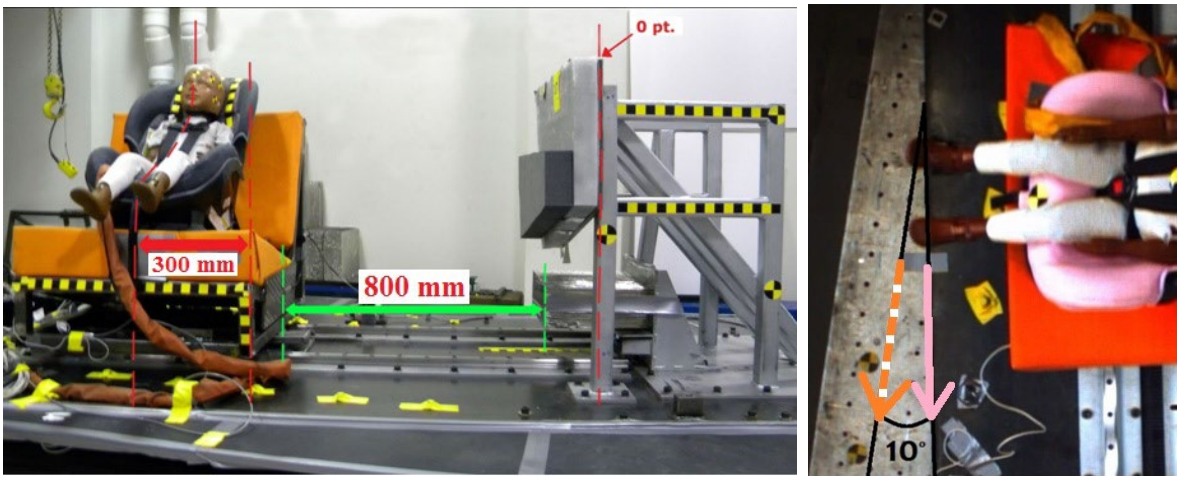

Figure 11: Side impact fixture set-up showing the 800 mm distance between the initial position of the secondary sled and the aluminum honeycomb as well as the top view of the 10° angle

Assessing the results of a representative series of forward facing tests, DOT_SIDE_064 through _066, a coordinate system was established with the X-direction aligned with the head forward/rearward motion (flexion/extension) and the Y-direction aligned with the linear bearing rails (Figure 12). Tracking along the X-direction depicts the head forward displacement versus time (Figure 13). Time 0 was set by the impact of the primary sled to the decelerator. The time at which the secondary sled impacts the aluminum honeycomb was measured by a trigger switch set between the aluminum honeycomb face and the honeycomb impact plate. Note that the maximum X-displacement (Table 12) occurs prior to the secondary sled impacting the honeycomb (Table 13). The Y-Displacement aligns with the distance travelled along the linear rails since y=0 at Time 0.

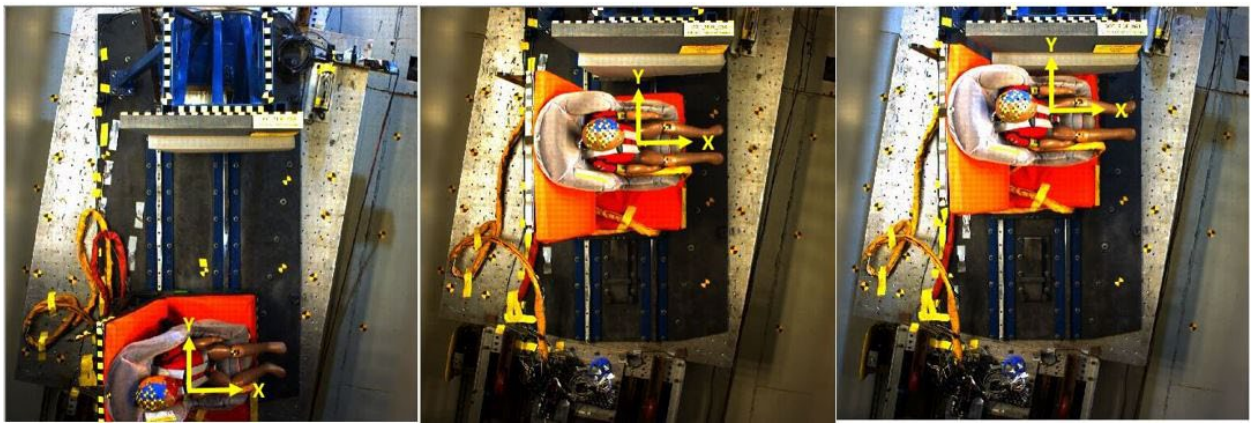

Figure 12: Forward Facing Q3s Graco Comfort Sport overhead view at Time 0, maximum X-displacement, and secondary sled impact with the aluminum honeycomb

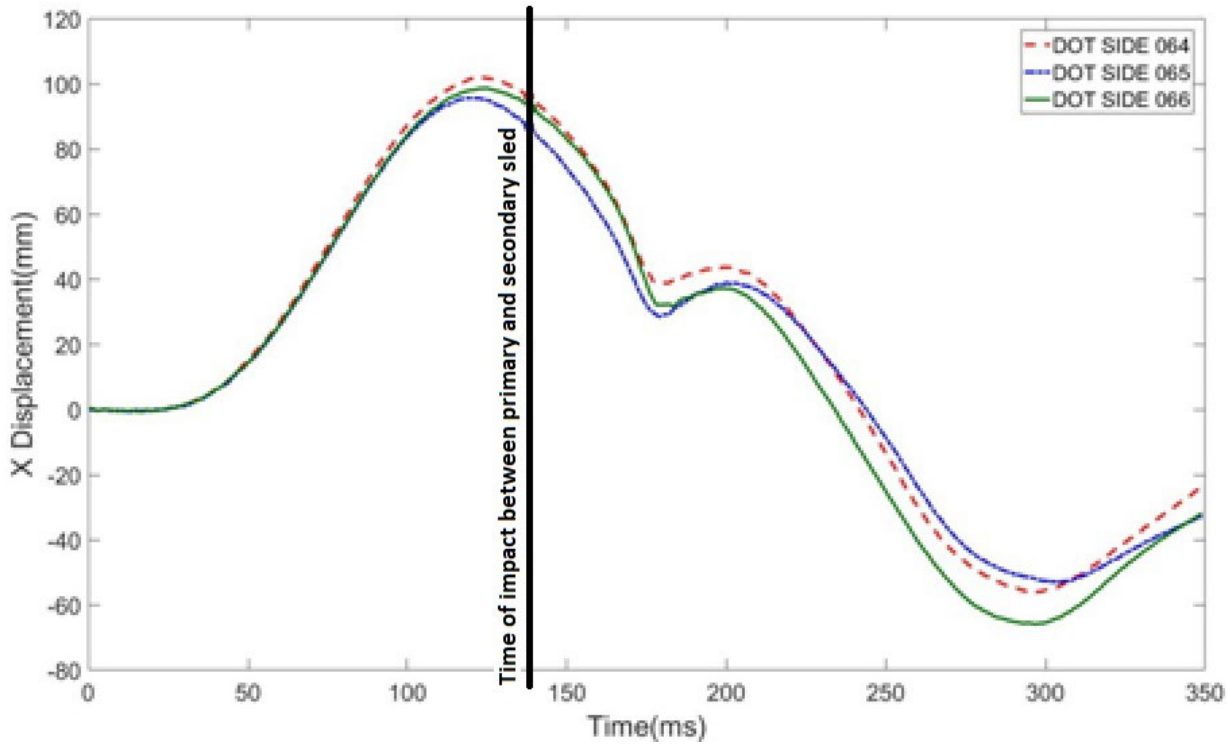

Figure 13: Forward Facing Q3s Graco Comfort Sport Head Excursion X-Direction

Table 12: Location of the top of the ATD head in the forward facing Graco Comfort Sport at maximum X displacement

Test Number	Orientation* (FF or RF) and ATD	Time at Max Head Displacement (msec)	Top of Head Location X-Direction (mm)	Top of Head Location Y-Direction (mm)
064	FF Q3s	124	102.0	723.8
065	FF Q3s	122	95.6	695.5
066	FF Q3s	125	98.6	720.7

Table 13: Location of the top of the ATD head in the forward facing Graco Comfort Sport, when the secondary sled impacts the aluminum honeycomb as defined by the trigger switch

Test Number	Orientation* (FF or RF) and ATD	Time at Secondary Sled Contact (msec)	Top of Head Location X-Direction (mm)	Top of Head Location Y-Direction (mm)
064	FF Q3s	138	96.1	849.2
065	FF Q3s	138	86.9	837.1
066	FF Q3s	139	92.4	845.0

* Forward Facing (FF) or Rear Facing (RF)

During the 800 mm run-up, the head nodded forward and begun moving back toward the CRS seatback. Therefore, when the secondary sled contacts the honeycomb, the head contacts the side wing of the CRS and, due to momentum, continues the rearward trajectory. If the run-up between Time 0 and the impact of the secondary sled with the aluminum honeycomb was shorter, the ATD head could be in a different position and moving in a different direction (forward versus rearward). If, at impact with the honeycomb, the head was moving forward, the momentum of the ATD head would continue to move the head forward at contact with the side wing. The kinematics of the ATD could vary not only with respect to different CRS and CRS orientation, but also with respect to the test setup and the run-up distance from Time 0 to honeycomb impact. Therefore, the run-up dimensions, head position and direction of motion could be sources of variability.

4.4 ATD Damage Analysis

The Q3s ATD exhibited lower extremity deformation at the conclusion of this test series (Figure 14). It is noted that deformation/misalignment is evident in the hip (green) as well as the knee (blue) joints.

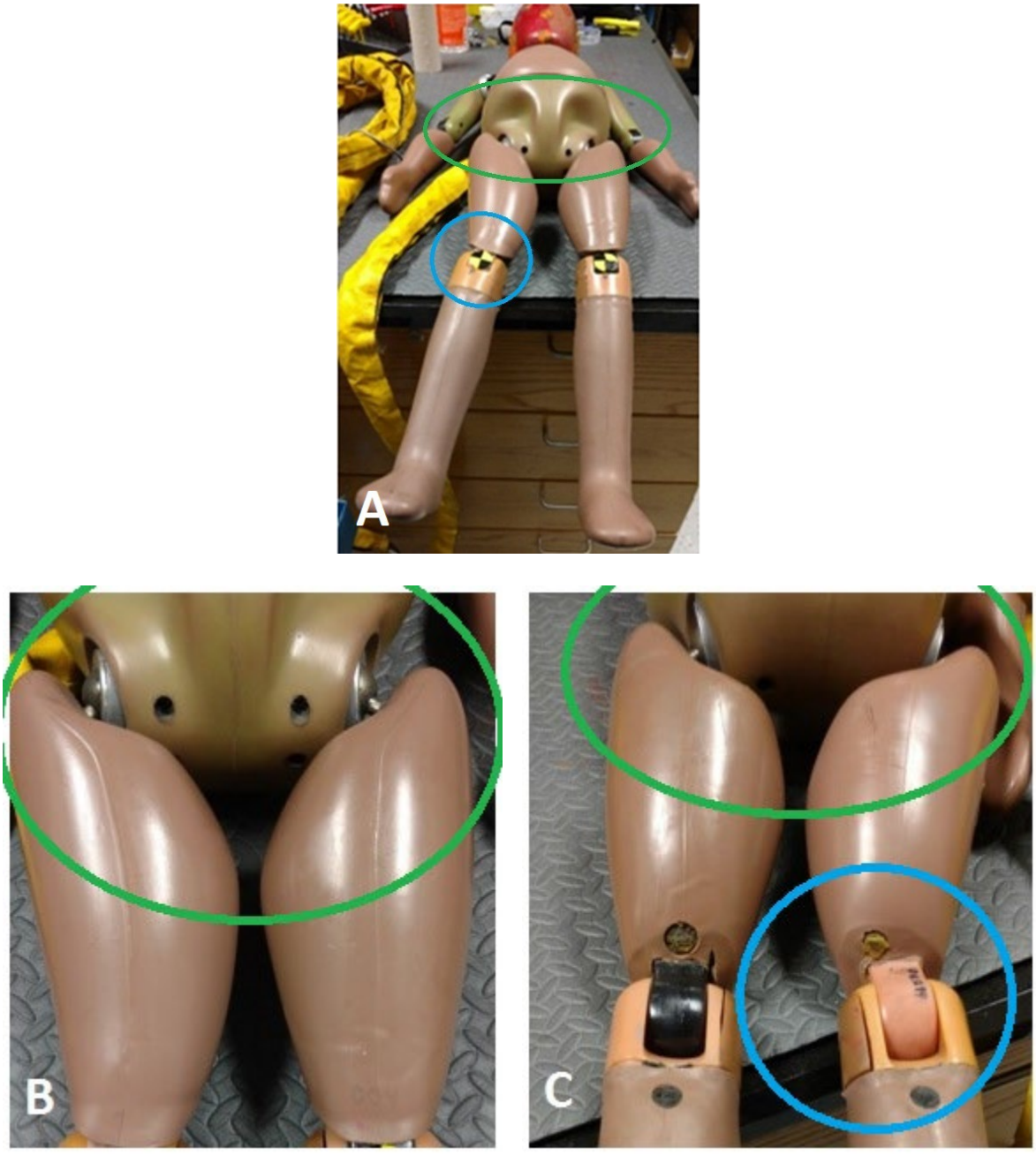

Figure 14: Views of post test Q3s lower extremities including A) overall, B) front, and C) rear view

The Q3s ATD also exhibited deformation of the "Nose Spring Ball Plunger" (Figure 15) in the left shoulder joint. This part assists in keeping the arm at the proper angle during set-up and test. It is advised to keep extra parts on hand during the test series and replace as needed.[7]

Figure 15: "Nose Spring Ball Plunger" Humanetics P/N 9003792-FT

During test DOT_SIDE_071 utilizing the rear facing CRABI 12, the right arm elbow joint connection tab broke during the side impact test (Figure 16). Since the connection tab is molded into the upper arm piece (Figure 17) and could not be repaired or replaced, a new replacement upper arm was purchased at a cost ~$1100. If the CRABI 12 is going to be used in standard side impact testing and subjected to multiple impacts to the arms (both rear and forward facing), the connection tab integrity could benefit from metal fabrication.

Figure 16: Screen shot from test DOT_SIDE_071 showing post impact elbow break

[7] The part, Humanetics #9003792-FT, is less than $20 as of June 2017.

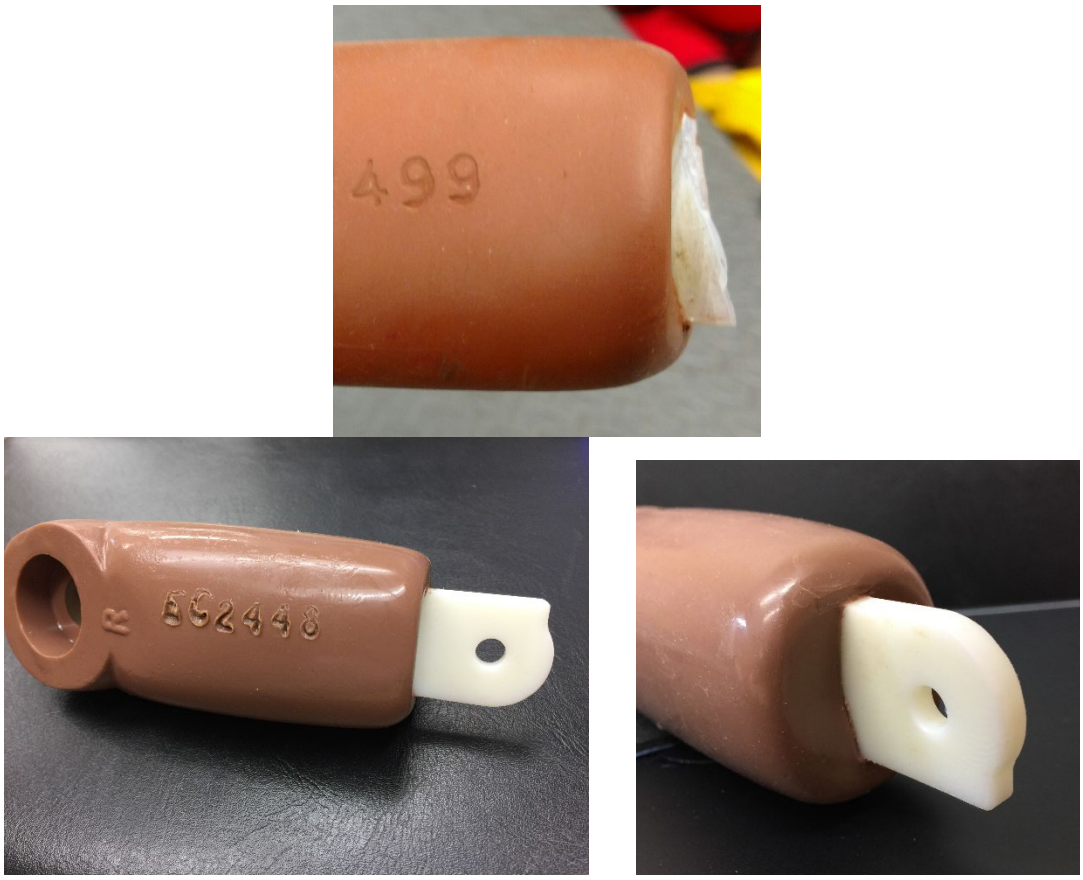

Figure 17: CRABI 12 right upper arm with both a broken and intact elbow connection tab

4.5 Seat Bight Gap

When installing the CRS for the first rear facing side impact test, DOT_SIDE_068, difficulties arose with the engagement of the Graco Comfort Sport CRS front structure with the seat back cushion (Figure 18). In order to install the CRS with the appropriate belt tension on the lower anchors, the front of the seat must engage the seat back cushion (Figure 19A). Also for appropriate installation, the CRS must be rotated so that the integrated ball level is in place. With the seat back at the appropriate angle to align the integrated ball level, the front seat structure initially fell below the seat back cushion (Figure 19B) into the seat bight gap.

It was confirmed that the pieces of the secondary sled seat structure were manufactured to the drawing specifications; the assembled KCS fixture was 18 mm higher in overall height than the drawing specifications (783 mm versus 765 mm, Figure 20). Since the positioning of the seat back foam is referenced from the top edge of the seat frame and the KCS seat back foam was placed per the drawing specifications, the gap between the seat bottom and the lower edge of the seat back was 18 mm larger than the design intent (KCS 88 mm versus NHTSA/VRTC 70 mm). With the seat bight gap 18 mm larger than that of the NHTSA/VRTC, the CRS front structure would not engage the seat back cushion Therefore, to conduct the rear facing CRS tests, the seat back foam was moved downward, closing the gap, by rotating the foam backing plate

180 degrees and shifting the placement of the foam on the foam backing plate. The seat bight gap for Tests 068 through 079 was 68 ± 2 mm. For Tests 061 through 067, which are forward facing, the seat bight gap was 88 mm.

To reduce the chance of CRS rear facing installation issues, the drawing package could benefit from the specification of the seat bight gap measurement of 70 mm or less.

Figure 18: Graco Comfort Sport rear facing with adjusted seat back cushion location

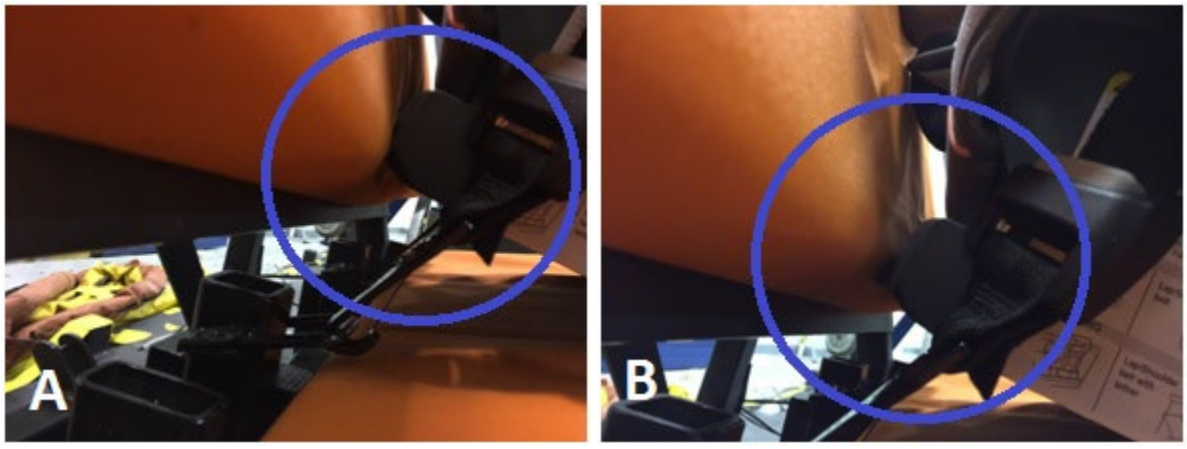

Figure 19: Close up view of the rear facing seat bottom showing A) engagement with the seat back foam and B) loss of engagement with the seat back foam

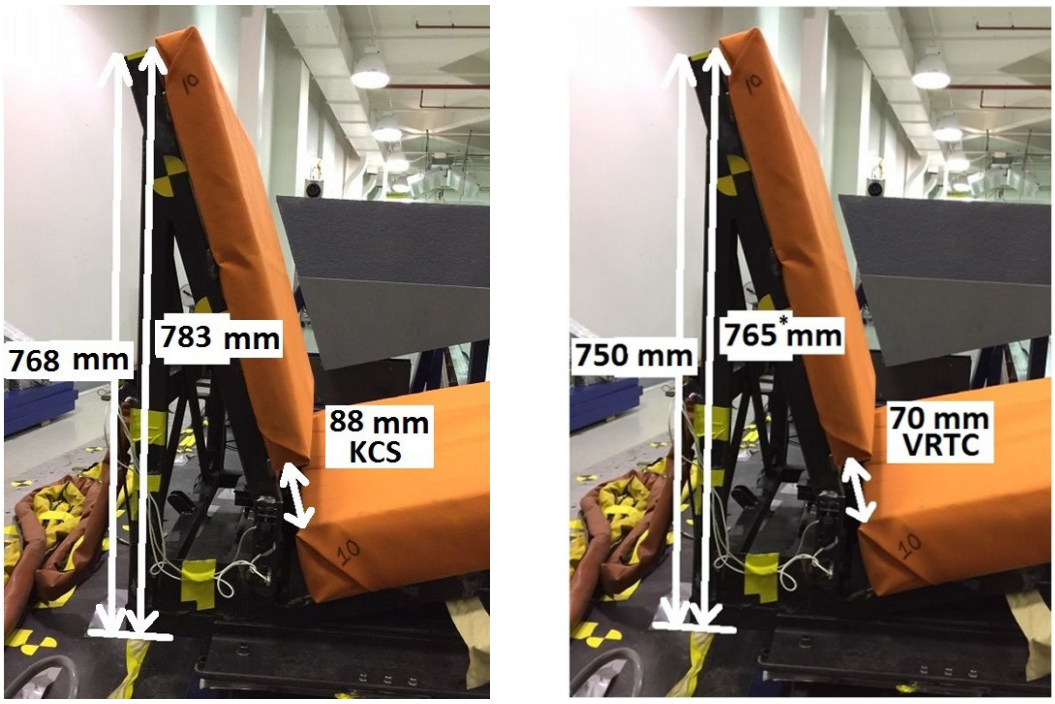

* Dimension equivalent to drawing package

Figure 20: Comparison KCS versus NHTSA/VRTC seat back cushion vertical dimensions

4.6 Assessment of the Linear Bearings and Push Testing Post-Series

During deceleration sled testing with the side impact fixture, when the primary sled impacts the decelerator, the secondary sled moves along the linear bearings (four sets) for 800 mm prior to impact with the aluminum honeycomb. During this run-up, the speed of the secondary sled decreases due to the friction of the linear bearings and the friction of the anti-rebound pedal on the Delron® plate on the lower portion of the Bearing Plate (Figure 21). The force to move the secondary sled on the linear bearings is directly related to the friction force. A quasi-static measure of the force needed to move the secondary sled on the linear bearings was conducted prior to the CRS specific test series and at the conclusion of testing. The results of the push tests are listed in Table 14.

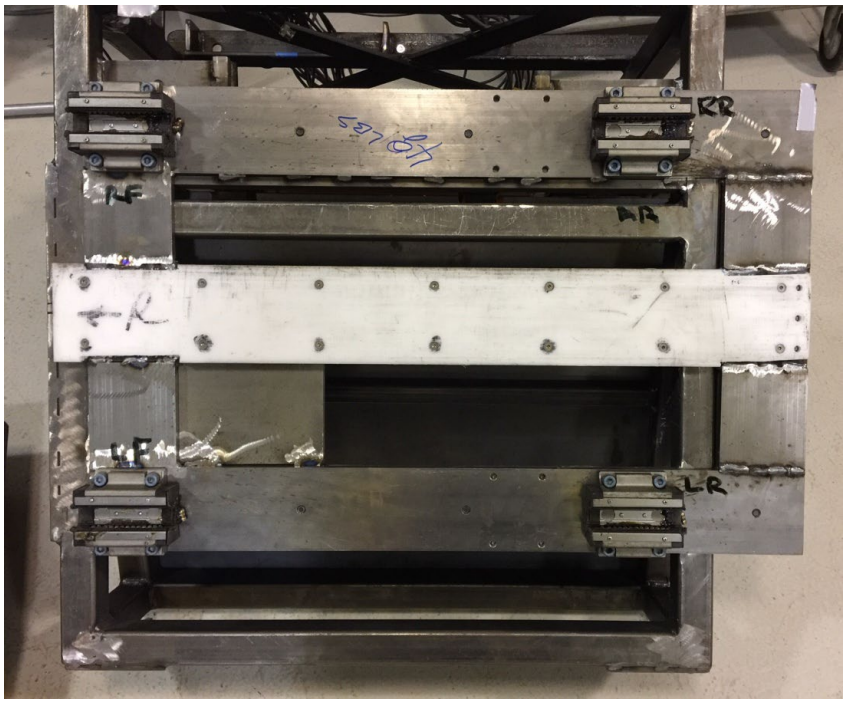

Figure 21: Bottom view of the bearing plate showing the four sets of linear bearings and the Delron® plate (white) that slides against the anti-rebound pedal

Table 14: Push force on the secondary sled to move it along the linear bearings

Push Test Description	Force Value (lb)
Push Test after fixture reconstruction prior to test DOT_SIDE_050: Over the anti-rebound pedal w/o lubrication	42 lb $\pm$ 1 lb
Push Test at conclusion of testing: Over the anti-rebound pedal w/o lubrication	43 $\pm$ 1 lb
Push Test at conclusion of testing: Over the anti-rebound pedal w/ lubrication	38 $\pm$ 1 lb
Push Test at conclusion of testing: No anti-rebound pedal	23 $\pm$ 1 lb

Since the friction force during the 800 mm run-up affects the ratio of the primary sled speed to the secondary sled impact speed, it is best to keep the friction force consistent from test to test. The force to push the secondary sled over the anti-rebound pedal without lubrication is 13% higher than with lubrication. Therefore, best practice would suggest a consistent method of either lubricating or not lubricating the pedal prior to every test so that the ratio of primary sled speed to secondary sled speed at impact remains predictable and consistent. Furthermore, if the anti-rebound pedal were to be removed altogether, the ratio of the primary sled speed and the secondary sled impact speed would not be dependent on the lubrication and could possibly reduce test speed variability.

While it is noted that the push force did not change between pre- and post- test series, it was beneficial to “tear-down” and inspect the linear bearings at the conclusion of the test series. A post test inspection of the bearings and the bearing rails showed:

- ✓ Both linear bearing rails were smooth to the touch, showing no visible signs of wear or roughness
- ✓ All four sets of bearings were well greased (A representative set of bearings are shown in Figure 22)
- ✓ All four sets of bearings rolled smoothly
- ✓ All four sets of bearings showed no visible deformation
- ✓ The bearing plate rolled off of and back onto the linear rails without binding

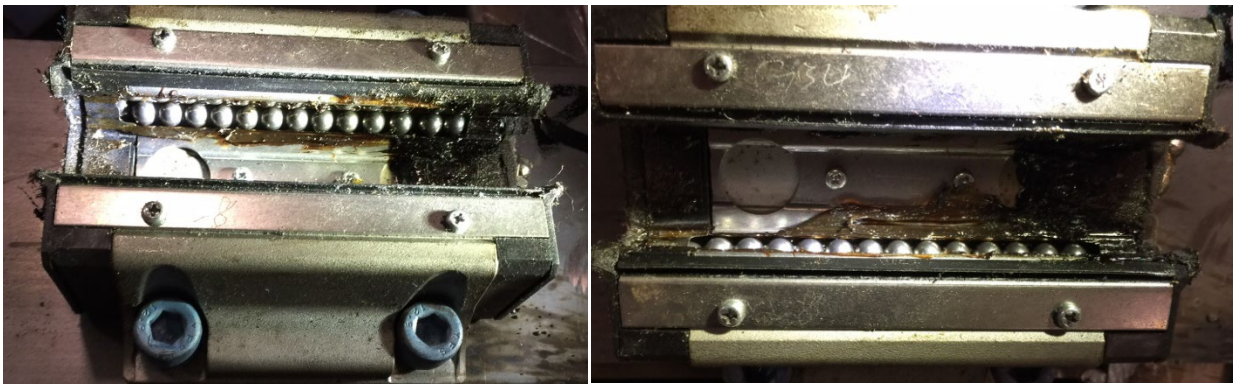

Figure 22: Inboard and outboard left rear linear bearings post test

5.0 Observations

The objective of Purchase Order DTNH22-15-P-00125 was to evaluate and compare kinematic/dynamic responses in side impact sled-on-sled tests in support of NHTSA's child restraint side impact test procedure development. Under the Purchase Order, eighteen (18) sled-on-sled side impact tests were conducted using the development test procedure to further demonstrate repeatability on a decelerating sled system. The decelerating sled system was also used to demonstrate reproducibility with comparable NHTSA/VRTC acceleration sled tests.

The following observations were discerned during the study:

- ✓ Deceleration sled testing was repeatable

Eighteen (18) CRS specific tests were conducted on the deceleration sled in seven (7) unique combinations of CRS, ATD, and seat orientation. For all reported tests, the acceleration pulse for the secondary sled fell within the prescribed corridor for at least two of the three measured positions.

From the Q3s, the HIC15 measures for each unique test combination reported less than 5% coefficient of variation.

From the Q3s, the Chest Y Displacement measures in the forward facing orientation for each unique CRS reported less than 5% coefficient of variation.

From the Q3s, the Chest Y Displacement measures in the rear facing orientation for each unique CRS reported 15% to 16% coefficient of variation.

For all CRABI 12 unique test combinations of CRS and seat orientation, the head-to door contact reported "No Contact".

- ✓ Deceleration sled testing demonstrated reproducibility

The accelerations measured on the secondary sled in each position, fell within the corridor and were comparable to the accelerations measured at the NHTSA/VRTC.

The Q3s HIC15 and Chest Y Displacement were compared within each facility and overall. The coefficient of variation was calculated for each group. The overall coefficient of variation was less than 5% for both injury indices.

Head motion analysis was completed for the deceleration sled CRS specific tests to be utilized for further study in reproducibility by NHTSA/VRTC. In the forward facing CRS orientation, the results indicated the head reaches a maximum forward position and begins to rebound back toward the seatback when the secondary sled contacts the aluminum honeycomb. Therefore, both head position and direction of motion could be sources of variability.

- ✓ Miscellaneous test issues

The CRABI 12 elbow joint broke on the impact side. The plastic connection tab integrity could benefit from metal fabrication

The Q3s displayed post test damage/misalignment to the structure of the hip as well as the knee joints.

A post test inspection of the bearings and the bearing rails showed no excessive wear, binding, or degradation.

Pull tests conducted on the secondary sled indicated different values of force needed if the anti-rebound pedal is engaged and if it has been lubricated. To remove variability with friction on the secondary sled during run-up, it is recommended to remove the anti-rebound pedal if possible.

The fixture seat bight width should be defined on the drawing package since an opening larger than 70 mm can affect the ability to properly install a rear facing CRS.

Appendix A: Fabrication of the Secondary Sled

The KCS side impact test fixture was constructed based on previous testing conducted with NHTSA[8]. The fixture was reconfigured as defined herein to align with the design intent of the NHTSA/VRTC fixture, accommodate use on the KCS deceleration sled, and address fixture changes requested by NHTSA/VRTC during the test series.

A.1 List of Fixture Modifications

Seventeen (17) issues were identified on the KSC fixture for reconfiguration. Of those, seven (7) design variations (in orange) were necessary to accommodate the fixture on the KSC deceleration sled. The remaining ten (10) fabrication changes were necessary due to various issues including:

- ✓ Clarifications/modifications on drawing dimensions from NHTSA/VRTC
- ✓ Structural additions from NHTSA/VRTC
- ✓ Modification needed to remove the ballast weight
- ✓ Fabrication variations from plans (i.e. bolts instead of welds, eliminated parts)

The complete list of the seventeen (17) identified issues included:

1. Base Plate (2921-100), length dimensions
2. Base Plate (2921-100), location of holes labeled "B" and "E" – Holes "B" were moved 267.2 mm reward from the design position or, with respect to the coordinate system on 2921-100, holes labeled B1 and B2 will have a XDIM of 120.2 mm instead of 387.4 mm. This accommodated the anti-rebound pedal deployment prior to honeycomb impact.
3. Impactor Frame and Stop Assembly (2921-200) – dimension change per NHTSA/VRTC (Figure A1)
4. Impactor Stop Assembly (2921-210) – alternate design
5. Door height change drawing 2921-240 "Impactor Frame Assembly" – dimension change per NHTSA/VRTC (Figure A2)
6. Linear Rail (2921-252) – length dimensions
7. Z-Point Plate (2921-305) – added per drawing dated February 2016
8. Bench Frame Assembly (2921-310) - additional tube, ballast, and ballast holder structure were removed
9. Bench Stop Plate (2921-322) – not used
10. Bench Seat Panel (2921-360) and Bench Seat Back Panel (2921-380) – Bench Seat Bottom and Back Panels were welded in place per drawing dated February 2016
11. Bench Frame Center Stiffener Plate (2921-314) – added per drawing dated February 2016 (Figure A3)
12. Seat Bottom and Back Cushion Mounting Plates (2921-371-1 and 2921-391-1) – Seat Bottom and Back Cushion Mounting Plates were fabricated in steal replacing the aluminum plates per drawing dated February 2016

[8] Brelin-Fornari, J., & Janca, S. (2014). *Development of NHTSA's Side Impact Test Procedure for Child Restraint Systems Using a Deceleration Sled: Final Report, Part 2* (No. DOT HS 811 995).

13. Bearing Mount Plate Assembly (2921-395) - The Bearing Mount Plate Assembly (2921-395) was manufactured per a new set of drawings generated by KCS and supplied to NHTSA/VRTC. Description of the modified Bearing Mount Plate Assembly is in Section A.2 “Bearing Plate Fabrication with Modified Bearing Locations”.
14. Anti-Rebound Fixture Assembly (2921-400) – alternative spring properties
15. Anti-Rebound Fixture Assembly (2921-400), Anti-Rebound Fixture Guide (2921-403) – alternative design needed for sliding clearance
16. Left and Right Side Bumper Assemblies (2921-410 and 2921-420) – not used
17. Stiffener Bar – no part number, part added per NHTSA/VRTC (Figure A3)

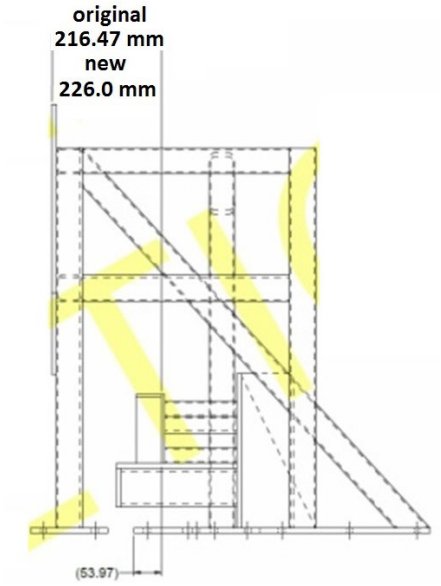

Figure A1: Dimension change on Impactor Frame and Stop Assembly (2921-200)

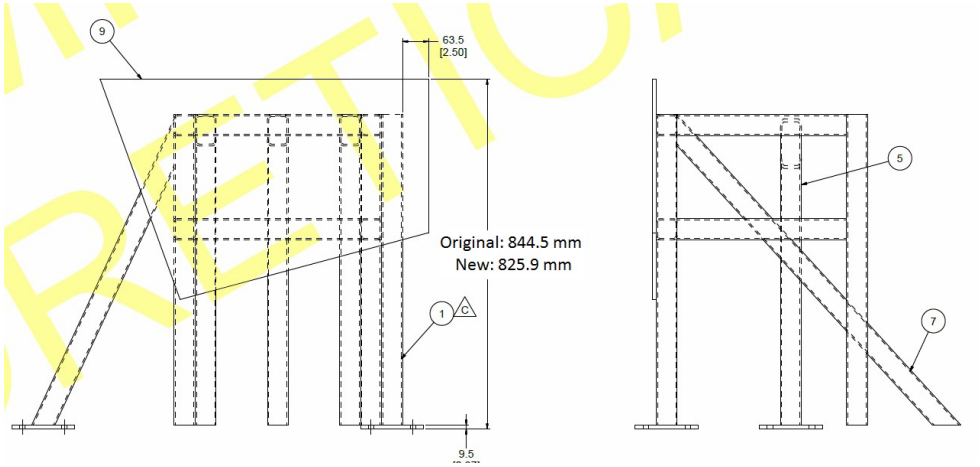

Figure A2: From drawing 2921-240 “Impactor Frame Assembly” depicting the adjusted height of the Impactor Door Plate

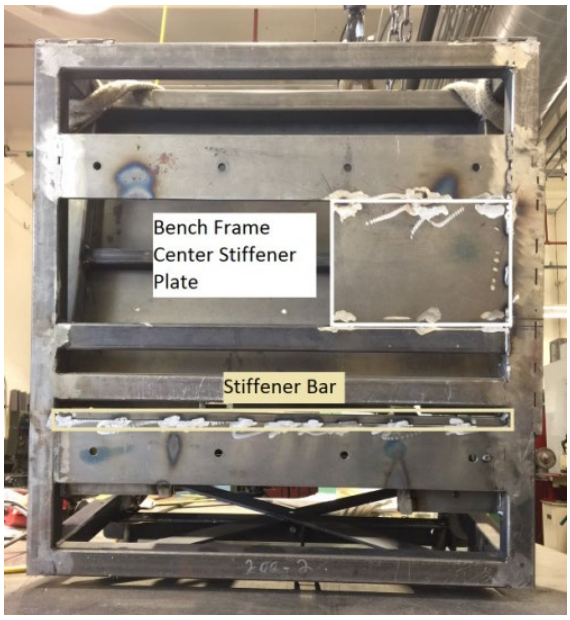

Figure A3: Bench Frame Assembly (2921-310) bottom view showing outlines of the Bench Frame Center Stiffener Plate (2921-314) and the Stiffener Bar

With the design changes, the total weight of the secondary sled Bench Assembly (2921-300) was 295. lb (Table A1). The overall weight of the Bench Assembly without a ballast weight, prior to the structural modifications, was 267 lb.

Table A1: Weight of Bench Assembly (2921-300)

Part	Weight (lb)
Bench Frame Assembly (2921-310) without Bench Base Mtg. Angle (2921-312)	214.
Bearing Mount Plate Assembly (2921-395) with four (4) attached flange type – heavy load sliders	48.
Bench Base Mtg. Angle (2921-312)	8.5
Seat Back Cushion Assembly (2921-390)	12.
Bottom Seat Cushion Assembly (2921-370)	12.5
Total Weight of Bench Assembly (2921-300)	295.

A.2 Bearing Plate Fabrication with Modified Bearing Locations

The Rail Bearing Mount Plate (2921-396) is designed as a one piece part. With four bearings attached, the part rides on the linear bearing rails attached to the primary sled (Figure A4). The secondary sled bench then attaches to the top side of the plate. While the Rail Bearing Mount Plate (2921-396) can be precision cut and CNC machined, it still may be difficult to properly align the plate with the linear bearing rails attached to the primary sled. In order to properly fit the Rail Bearing Mount Plate to the linear rails, the plate was constructed of four individual pieces (Figure A5) welded together in place on the rails. This process eliminated any issue with

the bearings being misaligned from side-to-side yet corresponded with the design intent of the Rail Bearing Mount Plate.

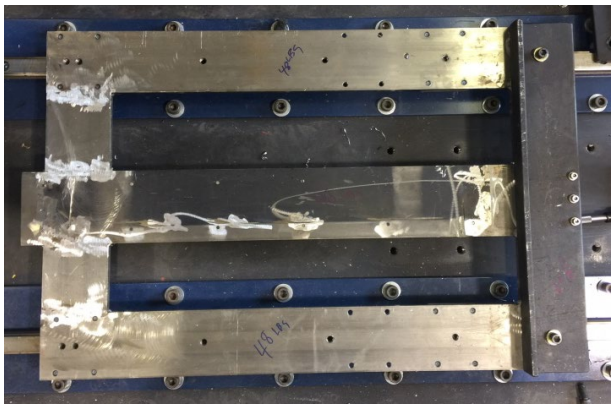

Figure A4: Bearing Mount Plate Assembly with Bench Base Mtg. Angle

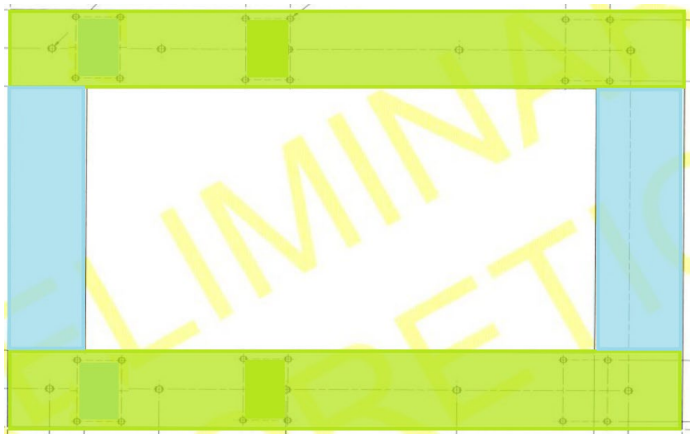

Figure A5: Fabrication of the Rail Bearing Mount Plate (2921-396) as four (4) individual parts (two green and two blue) welded together as one

KCS was informed that the Bench Bearing Support Plate (2921-313), which attaches to the Rail Bearing Mount Plate (2921-396), showed signs of bowing on the NHTSA/VRTC fixture. Bowing was also noted on the KCS, denoted in Figure A6 with red hashed lines on the Bench Bearing Support Plate. It was suspected that the bowing occurred due to the welding of the Lower Anchor Support Plate Spacer Bars (2921-712) to the Bench Bearing Support Plate. The yellow ovals in Figure A6 highlight the bottom side of the welded areas. In the current drawing package, the bearings are placed where the green rectangles are located in Figure A6. KCS relocated the bearings (Figures A6 and A7 blue rectangles) for the following reasons:

- ✓ More even distribution of weight on each bearing
- ✓ Increased support of the structure on the acceleration measurement end, reducing a possible cantilever effect of the structure (and subsequent oscillations due to impact)
- ✓ Bearing placement outside of the area where bowing may occur (due to fabrication) thus reducing the risk of the bearings binding due to misalignment

The updated drawing for the Rail Bearing Mount Plate (2921-396) is shown in Figure A8.

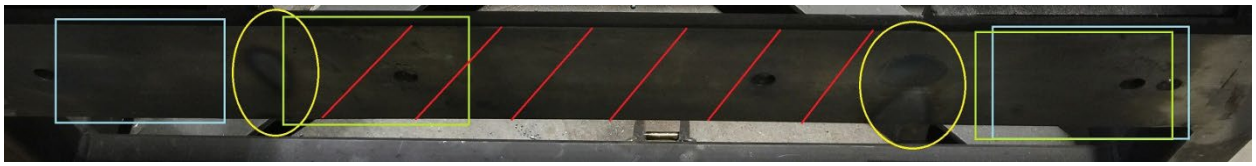

Figure A6: The Bench Bearing Support Plate (2921-313) depicting the area of bowing (red hashed lines), location of Lower Anchor Support Plate Spacer Bars (2921-712) welds (yellow ovals), and current location of the bearings for NHTSA/VRTC (green rectangles) and KCS (blue rectangles)

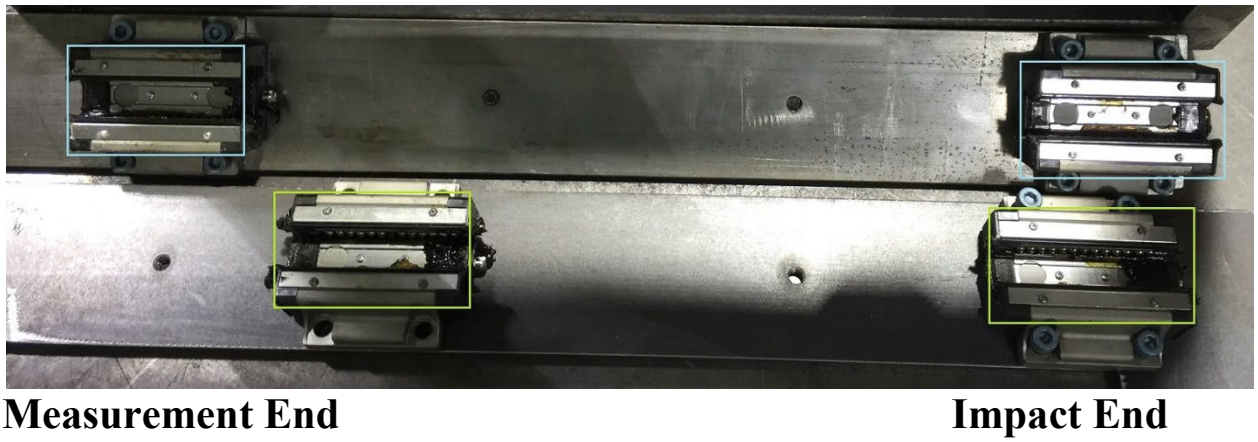

Figure A7: Side-by-side comparison of the KCS (blue) and design intent (green) bearing locations on the Rail Bearing Mount Plate (2921-396)

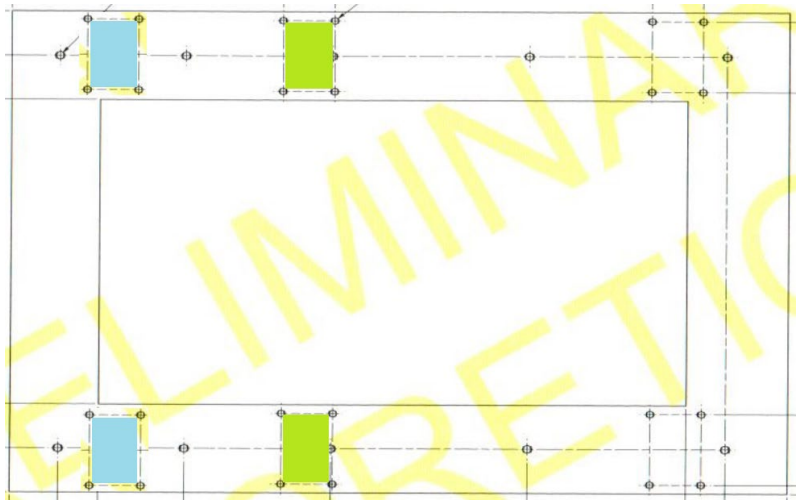

Figure A8: Rail Bearing Mount Plate (2921-396) showing the relocation of bearing attachments from the current drawing green position to the blue position

Appendix B: Secondary Sled Acceleration Pulse Evaluation

A series of side impact tests were conducted (Table B1) to assess variations to the secondary sled acceleration pulse with respect to:

- ✓ Accelerometer placement and models
- ✓ Weight of the secondary sled
- ✓ Aluminum honeycomb properties and dimensions
- ✓ Secondary sled structure

All tests were conducted with:

- ✓ Forward facing Graco Comfort Sport CRS
- ✓ Un-instrumented Hybrid III Three Year Old (HIII 3YO) ATD

It was determined:

- ✓ The location of the accelerometer on the secondary sled affects the measured value of acceleration for a common input.

- ✓ An increase in secondary sled weight decreases the overall amplitude of the acceleration pulse and increases the duration of the pulse.

- ✓ An increase of aluminum honeycomb pressure properties (80 psi increased to 90 psi) increases the overall amplitude of the acceleration pulse and decreases the duration of the pulse.

- ✓ Small changes in dimension of the aluminum honeycomb results in a noticeable change in the secondary sled pulse. Sizing the aluminum honeycomb by the number of complete (active) cells may help ensure repeatability.

- ✓ The fabrication and structure of the secondary sled fixture affects the shape of the acceleration pulse.

- ✓ Deployment of the anti-rebound pedal affects the amplitude and duration of oscillations seen in the secondary sled acceleration response.

Table B1: Secondary Acceleration Pulse Evaluation Test Series

Test Number	Objective	Accel Position*	Secondary Sled Weight (lb)	Honeycomb Pressure (psi)
16-001	Initial Set-up (10 lbs ballast weight)	A	277	80
16-002	Decreased weight	A	267	80
16-003	Increased weight	B	315	80
16-004	Increased weight with 90 psi honeycomb	B	315	90
16-005	Target weight (NHTSA/VRTC weight) with 90 psi honeycomb	B	294	90
16-006	Repeat of Baseline 16-002 with altered fixture (Seat pans welded, anti-rebound pedal moved to deploy before secondary sled impact with wall, remove ballast weight, Z-pt plate added)	B	267	80
16-007	Repeat of Baseline 16-005 with altered fixture (Seat pans welded, anti-rebound pedal moved to deploy before secondary sled impact with wall, remove ballast weight, Z-pt plate added)	B	294	90
16-008	Honeycomb size: 13.5” x 4.5” w/ modified fixture	B	294	90
16-009	Honeycomb size: 13.5” x 4.5” w/ modified fixture	B	294	90
16-010	Honeycomb size: 13.5” x 4.25” w/ modified fixture	B	294	90
16-011	Honeycomb size: 13.5” x 4.0” w/ modified fixture	B	294	90
16-012	Honeycomb size: 13.5” x 4.25” w/ modified fixture	B	294	90
KETT-01	Comparison of Endevco A and E series accelerometers placed on the **primary sled**	C	N/A	N/A
KETT-02	Welded seat back and bottom plates, 27 lb ballast plate	D	294	80
KETT-03	Welded seat back and bottom plates, 27 lb ballast plate, anti-rebound pedal moved 4” rearward for 0.25” clearance prior to impact	D	294	80
KETT-04	Welded seat back and bottom plates, 27 lb ballast plate, anti-rebound pedal moved 8” rearward for 4.25” clearance prior to impact	D	294	80
KETT-05	Welded seat back and bottom plates, no ballast plate, anti-rebound pedal moved 8” rearward for 4.25” clearance prior to impact	D	267	80

* Accelerometer Position refers to the configurations in Figures B2 through B5

B.1 Accelerometer Placement and Model Variations

Four (4) different makes and models of accelerometers (Table B2) were utilized to measure acceleration in various positions/configurations on the right rear leg structure (Figure B1) on secondary sled (Figures B2 through B5).

Table B2: Accelerometers

Accelerometer Make and Model	Quantity	Index Number*	Serial Number(s)	Damped or Un-damped
Endevco 7290 E	2	1 2	35665 35667	Damped
Endevco 7231 C	1	3	AH446	Un-damped
Endevco 7290 A	2	4 5	33002 22605	Damped
PCB 3741E12200G	2	6 7	9641	Damped

* Index Numbers refer to labels on Figures B2 through B5

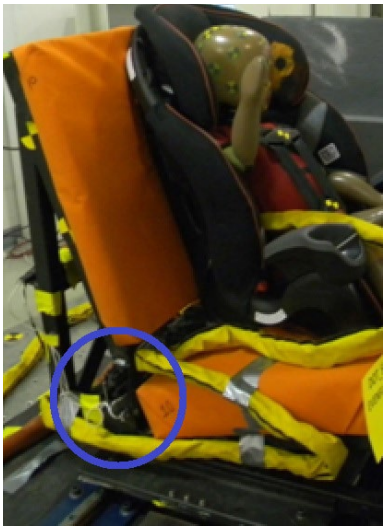

Figure B1: Location of accelerometers on right rear leg structure for configurations “A”, “B”, and “D” in Figures B2, B3, and B5

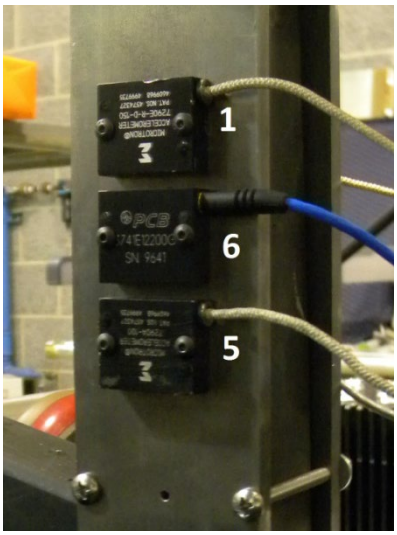

Inboard

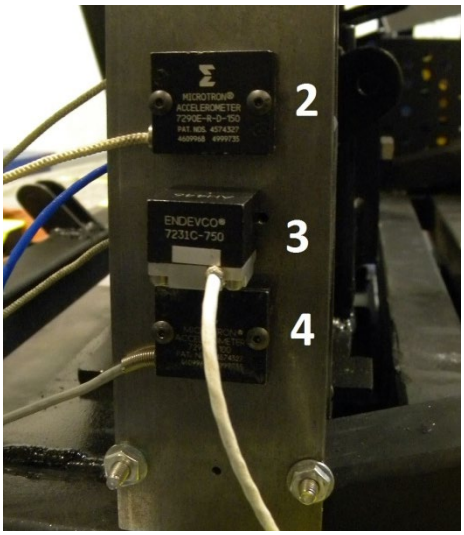

Outboard

Figure B2: Configuration “A” - Inboard and outboard accelerometer placement

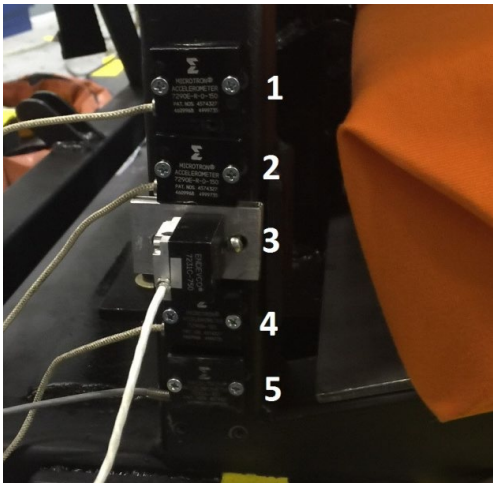

Figure B3: Configuration “B” – Outboard accelerometer placement

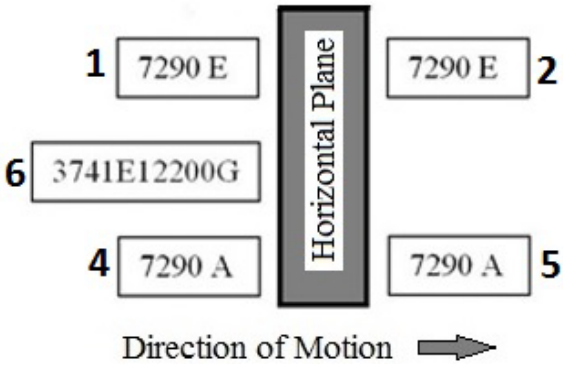

Figure B4: Configuration “C” - Overhead view depicting the location of the five (5) accelerometers on the primary sled with respect to each other and the direction of motion

Figure B5: Configuration “D” - Outboard accelerometer placement

It was noted that the accelerometer model and/or location on the secondary sled, affected the measured acceleration value (Figure B6).

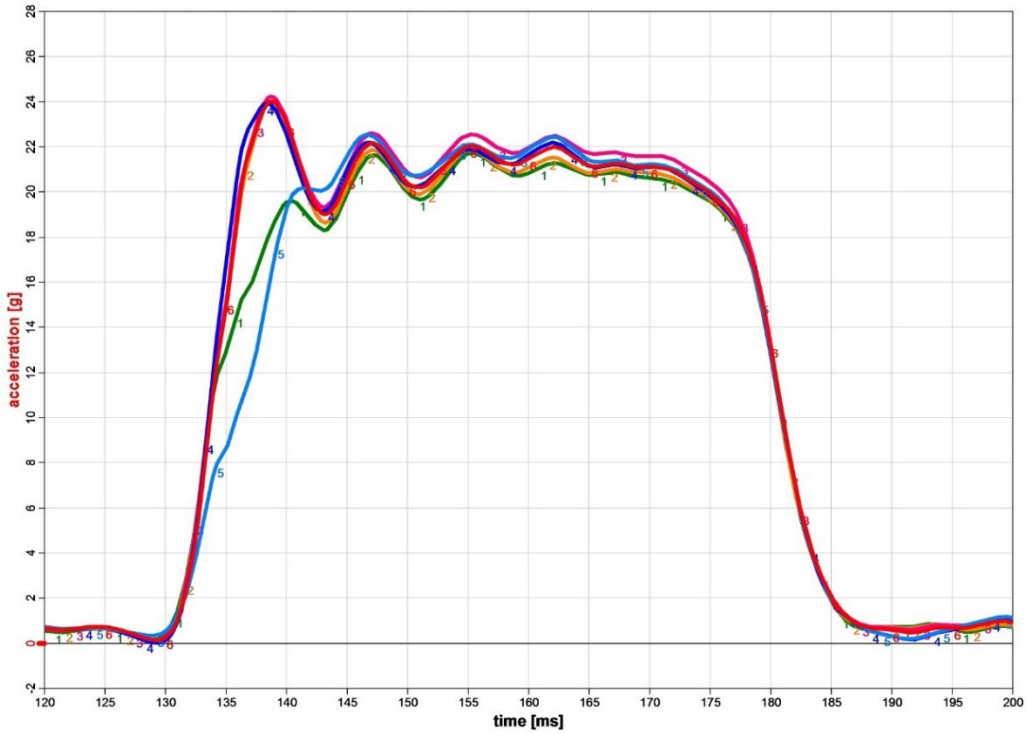

Figure B6: Secondary sled acceleration (Test 16-002) showing varying acceleration measures from various accelerometer models and locations with 80 psi honeycomb, 267 lb secondary sled weight, and a common input

To determine if the location on the secondary sled or the type/model of the accelerometer was causing the variation of the measured secondary sled acceleration pulse, Test KETT-01 was conducted with five (5) accelerometers rigidly attached to the **primary sled** (configuration "C"). The accelerometer placement was to a rigid mounting bracket on the primary sled which removed structural design issues that may be associated with the secondary sled. The "like" model Endevco accelerometers were mounted 180 degrees to each other in line with the direction of measurement. Therefore, for comparison purposes, the data was inverted for two accelerometers to represent negative acceleration for all measurements (Figure B7).

The acceleration measurements of the five damped accelerometers on the primary sled tracked and trended similarly for the complete test sequence (Figure B7). The greatest difference was in the magnitude of the peak deceleration with a difference of $\pm$ 0.2 g. Therefore, the difference in the acceleration measurements from the different accelerometer models observed in Baseline 16-001 through 16-005 was likely due to the location of the accelerometers on the structure of the secondary sled.

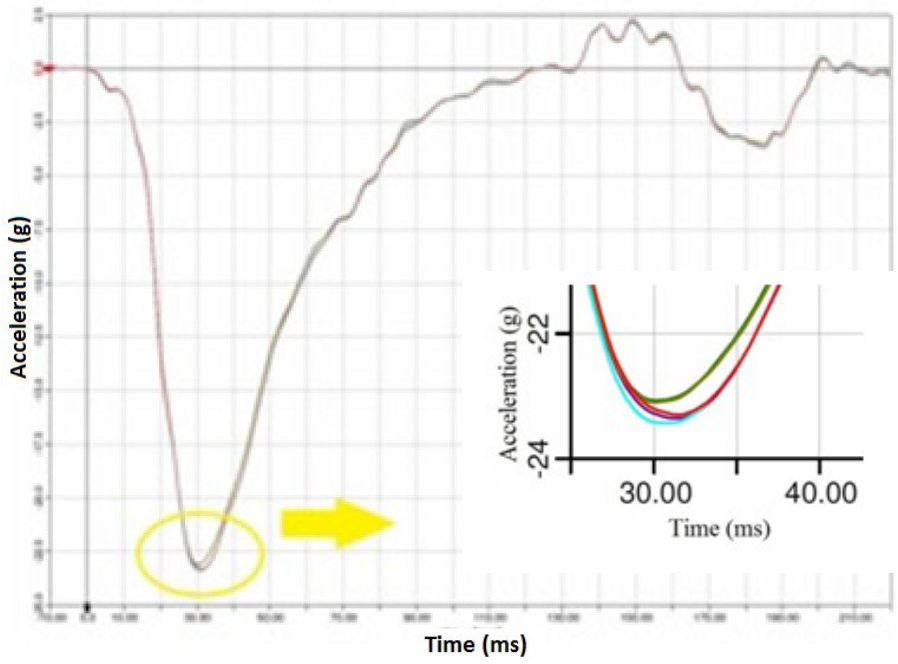

Figure B7: Acceleration measurement of the five (5) accelerometers on the **primary sled**

B.2 Secondary Sled Weight Variation

As the weight of the secondary sled increases, the amplitude of the acceleration decreases and the duration increases (Figure B8).

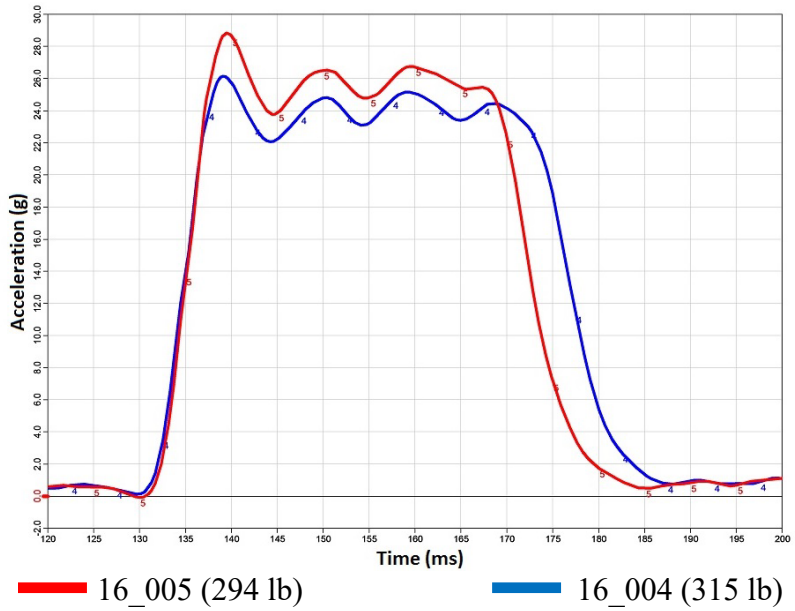

Figure B8: Secondary sled acceleration comparing secondary sled weight with 90 psi honeycomb

B.3 Aluminum Honeycomb Pressure and Size Variations

Using a consistent aluminum honeycomb test size of 12” (depth) x 13.5” (width) x 5.0” (length) and varying the pressure properties (80 psi and 90 psi), it was determined that an increase in aluminum honeycomb pressure increases the overall amplitude of the acceleration pulse and decreases the duration of the pulse (Figure B9).

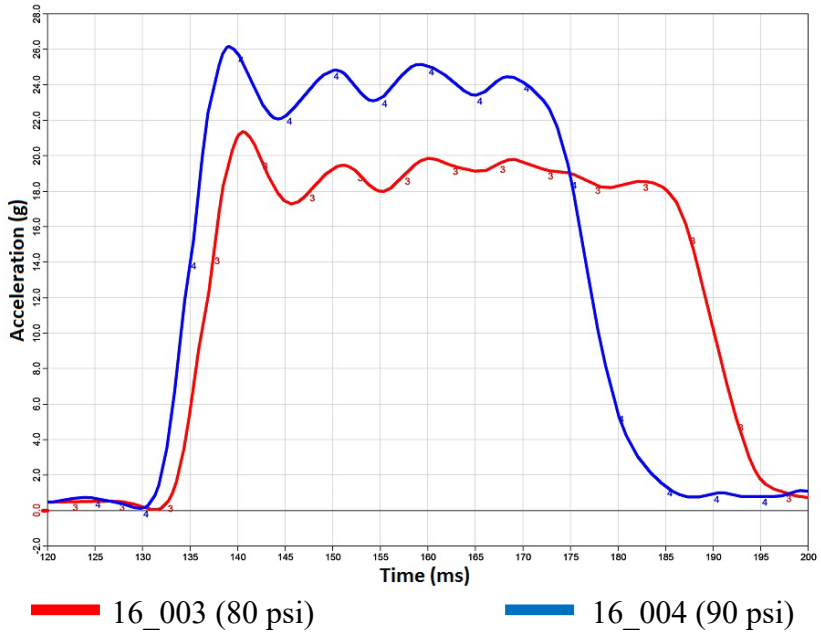

Figure B9: Secondary sled acceleration comparing 80 psi to 90 psi honeycomb with 315 lb secondary sled

Tests 16-009 through 16-011 assessed the variation of the impact area of the aluminum honeycomb block by 0.25” reduction in the block height for each test. It was determined that with a consistent secondary sled speed, a decrease in impact area (block height) decreases the acceleration pulse amplitude and increases the duration (Figure B10).

For the supplied sheet of 90 psi honeycomb, each cell was slightly smaller than 0.25”, therefore it was possible to either cut through a cell on each end (1/2 a cell on top and bottom) or have complete cells all the way across and still maintain the 4.25” dimension of material. The blocks could be18 or 19 cells tall by 50 cells across or 900 versus 950 total cells. The difference between the two variations is 5.5%. This could be enough to change the characteristics of the pulse: having a greater number of cells creates a stiffer pulse with greater amplitude and a shorter duration. Therefore, to ensure that the acceleration pulse of the secondary sled was consistent with respect to the size of the aluminum honeycomb, best practice suggests sizing by the number of complete (active) cells may be better for repeatability than sizing by dimensions (Figure B11).

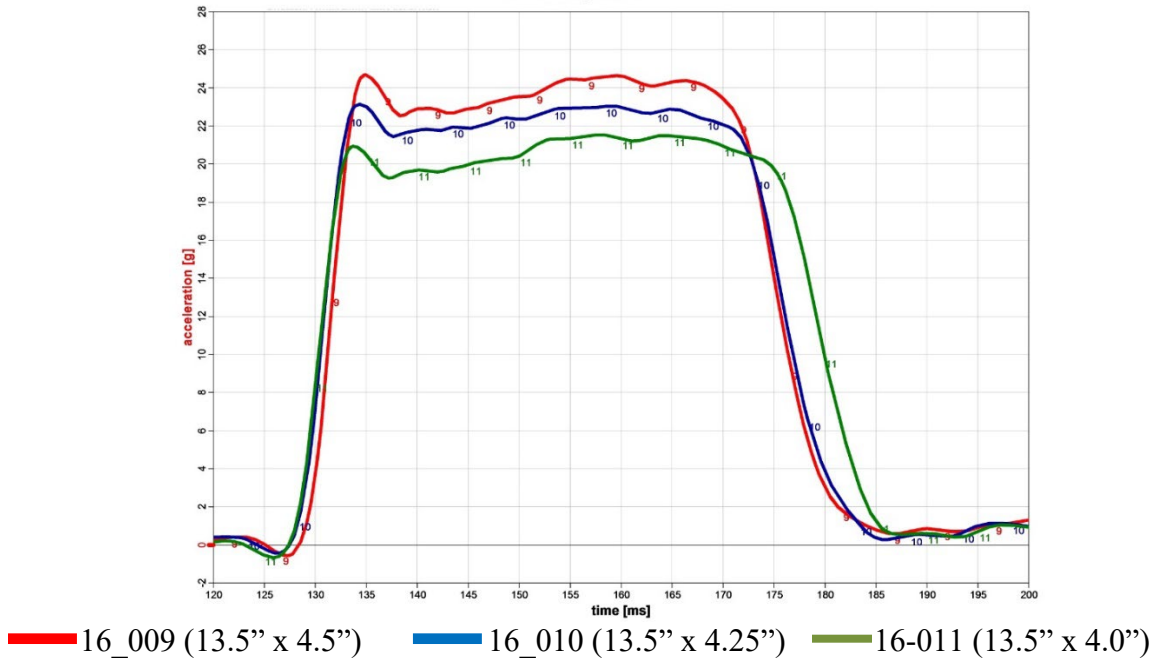

Figure B10: Comparison of Tests 16-009, 16-010, and 16-011

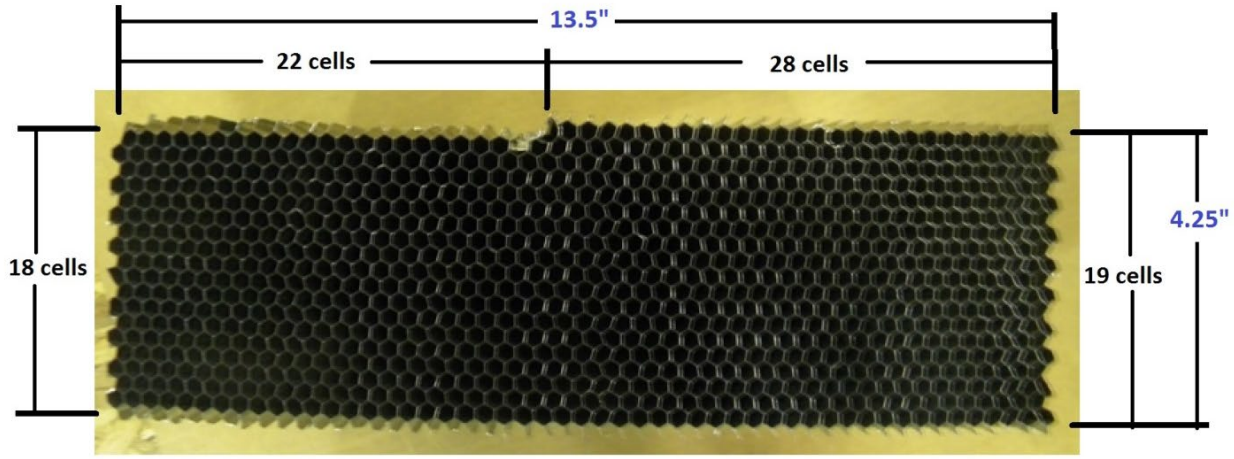

Figure B11: Honeycomb cut with 928 complete (active) cells

B.4 Secondary Sled Design Variations Effect on Acceleration Pulse

Structural variations were noted on the initial KCS fixture. Most were attributed to a ballast weight carrier designed into the fixture. A set of fabrication changes were conducted to assess the consequence of the variations on the acceleration pulse of the secondary sled. Changes included welding the seat pans to the fixture, removing the ballast weight, removing the anti-rebound pedal, and adding the Z-Plate. These changes reduced the amplitude of the oscillations of the secondary sled acceleration measurement (Figures B12 and B13).

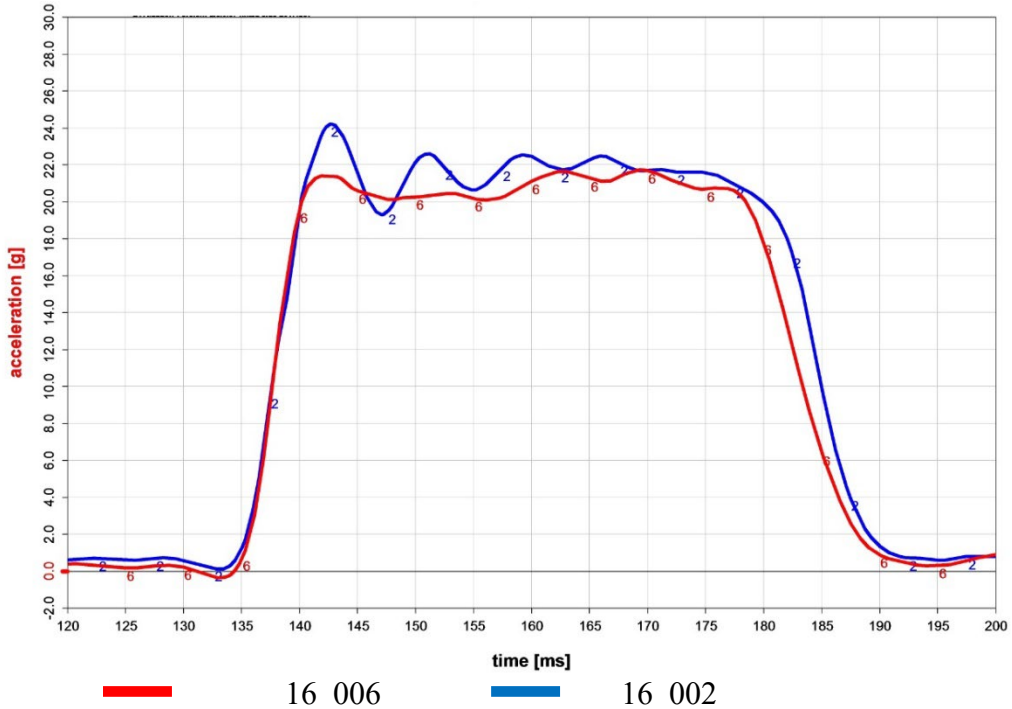

Figure B12: Comparison of secondary sled acceleration with (16-006) and without (16-002) specific fixture alterations

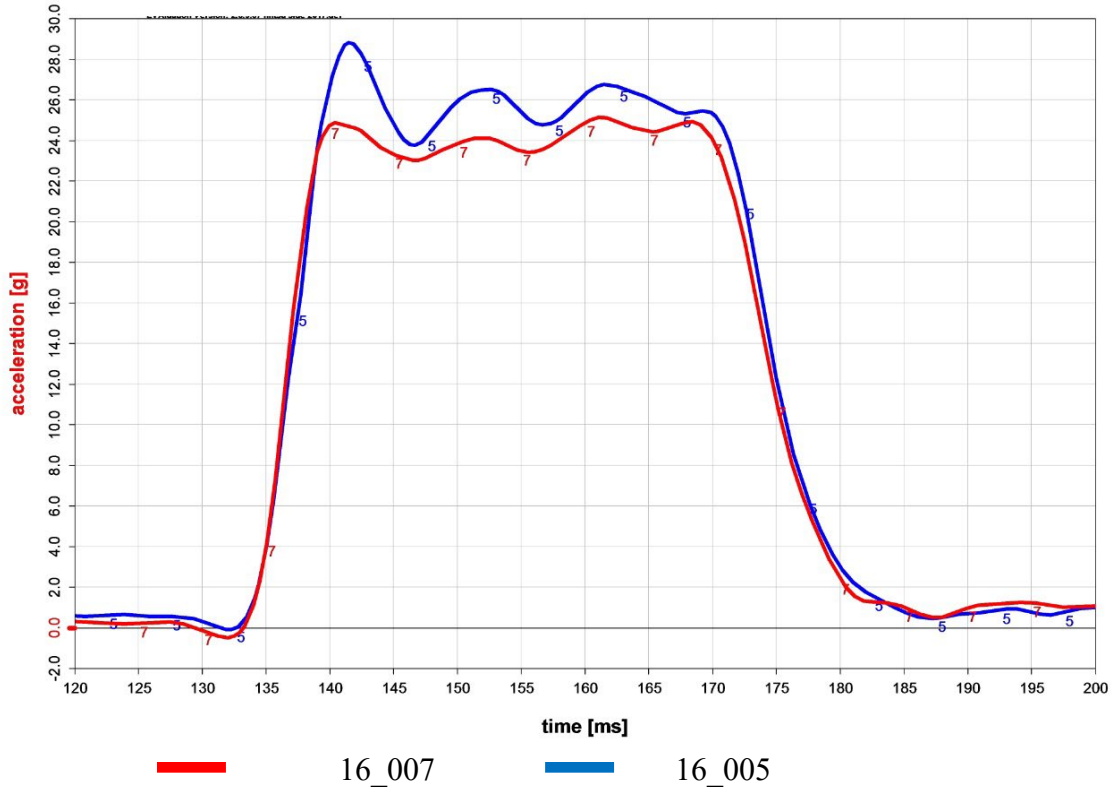

Figure B13: Comparison of secondary sled acceleration with (16-007) and without (16-005) specific fixture alterations

The intent of the Anti-Rebound Fixture Assembly (2921-400) is to halt the motion of the secondary sled once it impacts with the primary sled door assembly. The anti-rebound pedal rests on a set of linear springs which are depressed to allow the secondary sled to slid over it and then deploys (springs up) once the secondary sled has struck the primary sled. The anti-rebound pedal oscillates on the linear springs after it deploys. Tests were conducted to determine if the release of the anti-rebound pedal causes oscillations in the secondary sled acceleration pulse measurements. Testing was conducted with the anti-rebound pedal in the design location and with the anti-rebound pedal moved such that it deployed prior to secondary sled impact with the aluminum honeycomb. It was noted that the deployment of the anti-rebound pedal had some affect on the amplitude and duration of oscillations seen in the secondary sled acceleration response (Figure B14).

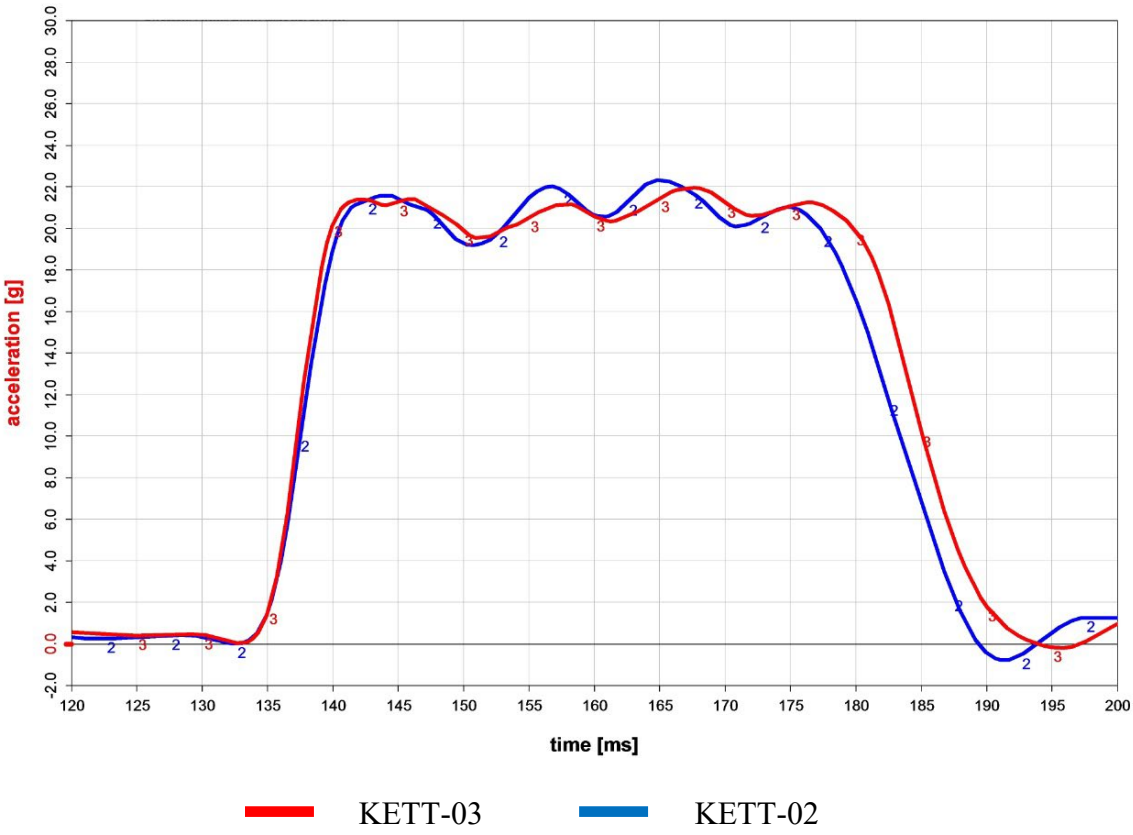

Figure B14: Comparison secondary sled acceleration with the anti-rebound pedal in the design location (KETT-02) and with the anti-rebound pedal deploying prior to secondary sled impact with the aluminum honeycomb (KETT-03)

Appendix C: KCS Deceleration Sled Side Impact Test Procedure

Initial Setup

The side impact fixture consists of two distinct parts: the primary sled and the secondary sled (Figure C1). The primary sled is fixed to the bedplate of the deceleration sled and consists of the fixture base plate, door fixture (with foams), and aluminum honeycomb. The secondary sled is free to move on a set of linear bearings affixed to the primary sled base plate at a 10 degree angle counter clockwise from longitudinal. The secondary sled consists of the generic vehicle seat (with foam and cover), the child restraint system (CRS) being tested, and the anthropomorphic test device (ATD). The (final) mass of the secondary sled is 133 kg (294 lbs). The fixture is constructed based on NHTSA drawing titled, "Child Side Impact Sled", February 2016.

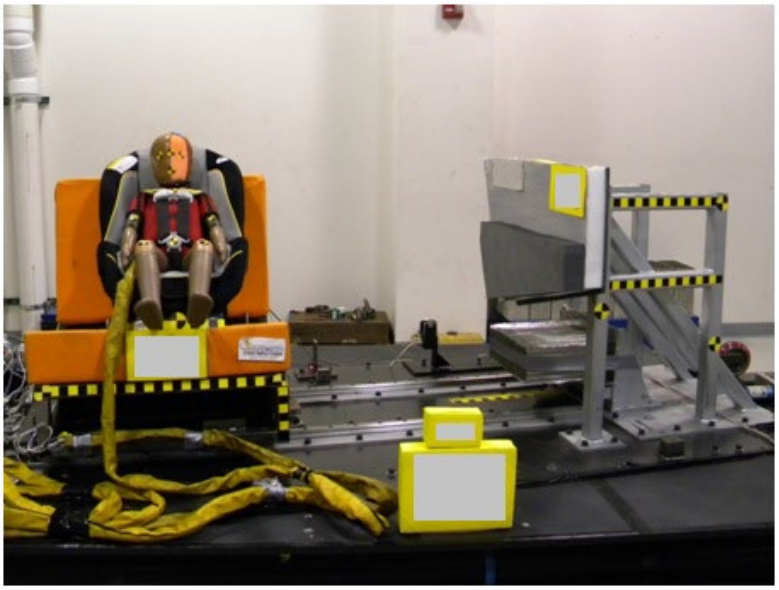

Figure C1: Front view of side impact fixture attached to the deceleration sled

Instrumentation: Fixture and Sled

The deceleration sled and the test fixture includes up to eight (8) channels of instrumentation (Table C1). Locations of the accelerometers on the test fixture are shown in Figure C2. All instrumentation is calibrated in accordance to the protocol specified in NHTSA "Laboratory Test Procedure for FMVSS No. 213, Child Restraint Systems" (TP-213-10 February 16, 2014) and SAE J211.

Table C1: Sled and fixture instrumentation

Position of Measurement	Type of Measurement
Primary Sled	Linear Acceleration
Secondary Sled Seat Base - Lower (along 10 degree)	Linear Acceleration
Secondary Sled Seat Base - Mid (along 10 degree)	Linear Acceleration
Secondary Sled Seat Base - Upper (along 10 degree)	Linear Acceleration
Top Tether (Forward Facing Only)	Axial Belt Load Force
Primary Sled Contact to Decelerator	Contact - Voltage
Secondary Sled Contact to Honeycomb	Contact - Voltage
Head Impact to Door (CRABI 12 only)	Contact - Voltage

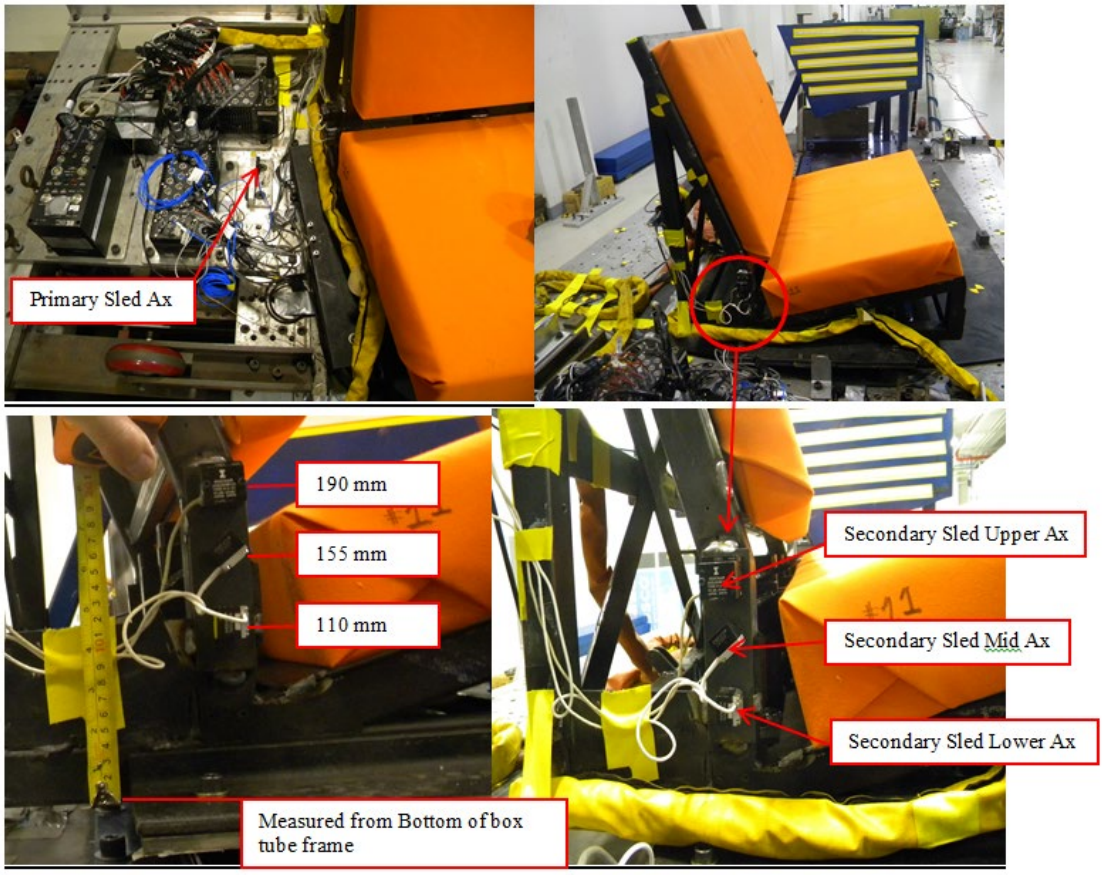

Figure C2: Accelerometer locations

Instrumentation: ATD

Two different ATDs are utilized in the side impact testing: Q3s and CRABI 12. The instrumentation for the ATDs is listed in Table C2. The instrumentation for the Q3s is calibrated according to the protocols specified in the NHTSA Notice of Proposed Rulemaking to incorporate the Q3s into Part 572 (49 CFR Part 572. November 21, 2013) and SAE J211. The instrumentation for the CRABI 12 is calibrated according to the protocols specified in NHTSA "Laboratory Test Procedure for FMVSS No. 213, Child Restraint Systems" (TP-213-10 February 16, 2014) and SAE J211. The CRABI 12 head is targeted for use in head motion analysis, covered in copper mesh for use with the door contact switch, and chalked for contact recognition. (Figure C3) The CRABI 12 is clothed as specified in TP-213-10.

Table C2: ATD instrumentation

Instrumentation Channel	**Q3s (number of channels)**	**CRABI 12 (number of channels)**
Head cg triax accelerometer	3	3
Neck upper load cell Forces Fy, Fz Moment Mx	3	3
Shoulder displacement Y	1	n/a
Chest triaxial accelerometer	n/a	3
IR-TRACC Displacement	1	n/a
Spine Y-axis accelerometer	1	n/a
Pelvis Y-axis accelerometer	1	1
Total	**10**	**10**

Figure C3: CRABI 12 heads prepared for testing with targets, copper mesh cover, and test chalk

The Q3s IR-TRACC measurement can be sensitive to the proper positioning of the abdominal covering. The placement of the Abdomen (Humanetics P/N 020-5000) should be checked prior to each test to insure that it is not tucked under the Rib Cage Assembly (Humanetics P/N 020-4018). (Figure C4)

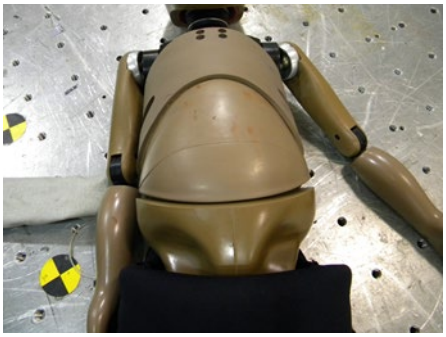

Proper Abdomen Placement (Untucked)

Improper Abdomen Placement (Tucked)

Figure C4: Proper and improper abdominal cover placement

High Speed Video and Photography

There are five (5) off board cameras specified for the side impact testing (Table C3). A layout showing the location of the cameras for forward facing and rear facing tests is provided in Figure C5. The camera speed setting is 1000 fps (frames per second) for all cameras.

Placards are attached to various positions on the fixture such that they can be seen in each camera view during the duration of the event. Placard information includes test number, child seat manufacturer and model, CRS attachment method, ATD type, and ATD position.

Table C3: Camera information

Camera	Camera Location	Lens
CAMOH	Overhead 1 (Wide View)	20 mm
CAM1	Overhead 2 (Tight View)	6 mm
CAM2	Front	12 mm
CAM3	In-Line with Secondary Sled	6 mm
CAM4	Door Surface (Rear Facing Only)	12 mm

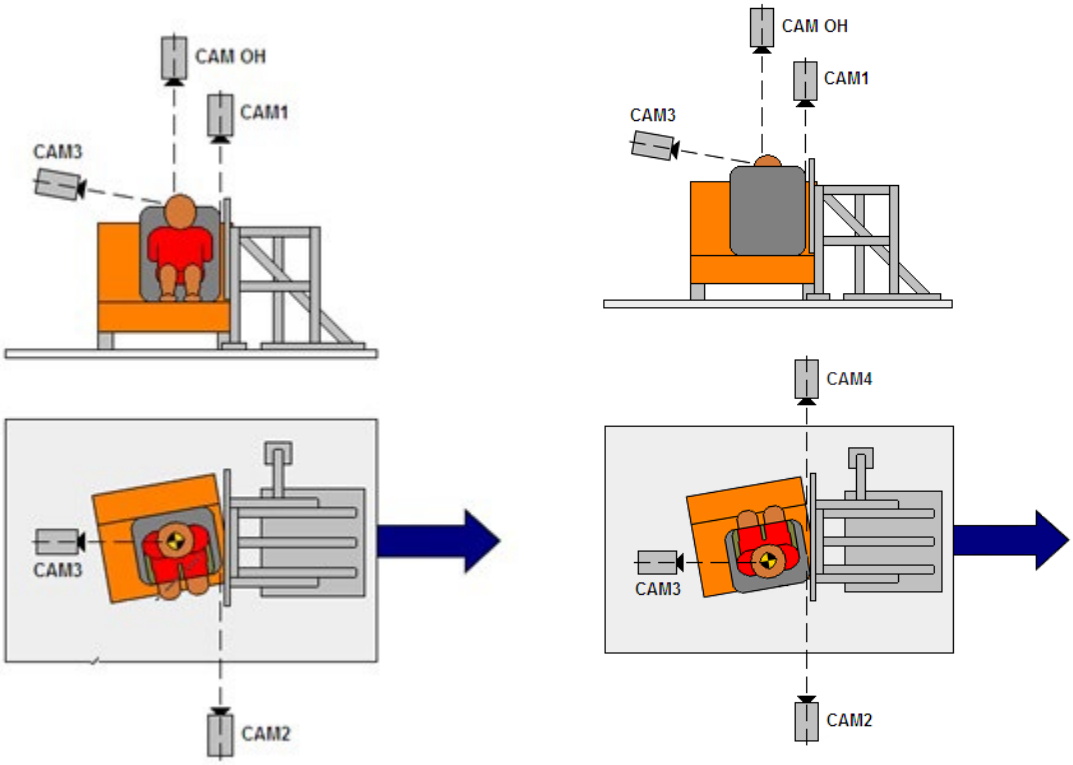

Figure C5: Layout of camera locations for forward facing and rear facing

Fixture and ATD Placement

- Fixture seat foam should be unloaded (allowed to rest) for a minimum of four (4) hours prior to testing. Fixture seat foam assemblies should be visually inspected after each test and replaced if needed.

- Position the secondary sled 800 mm ± 6 mm from the honeycomb impact surface (Figure C6).

- Apply inch tape and targets to the appropriate areas on the CRS for CMM pre-test measurements. According to the CRS Owner's Manual, adjust the internal harness and center buckle positions corresponding with the ATD size. Record the make, model, and serial number of the CRS.

- Position the centerline of the CRS on the sliding seat 300 mm ± 6 mm from the edge of the fixture seat, centered with the LATCH anchors. (Figure C6) Install the CRS per the Owner's Manual and ensure for rear facing CRS the seat inclination meets manufacturers' specifications.

- Install CRABI 12 with the upper arms aligned with the torso and the Q3s arm positioned in the detent. The hands set resting on the CRS seat cushion. Route the data umbilical along the side of the ATD leg (opposite of impact) between the CRS side interior and the ATD. Position ATD so that the torso is in contact with the back of the seat and the top of the head aligned with the center targets on the top and bottom of the CRS. Position the thighs so they are equally spaced from the buckle and contacting the CRS seat bottom. Buckle and tighten the CRS internal harness.

- Tighten the internal harness, lower anchor attachments, and (when applicable) the upper tether, according to installation guidelines in "Laboratory Test Procedure for FMVSS No. 213, Child Restraint Systems" (TP-213-10 February 16, 2014). Using a belt tension gauge, measure (and record) belt tension values for all three belt restraints. Target belt loads are listed in Table C4.

- Use a Coordinate Measurement Machine (CMM) such as a FARO arm to record measurements of the pre-test CRS, sled test fixture, and ATD position (see desired measurement positions in Table C5) to ensure test repeatability.

- Apply chalk/paint to the ATD's head. Use different colors to distinguish front, side, and top.

- Attach new door and armrest foam to the steel door frame using two sided tape. To ensure test repeatability, measure and compare the distance from the front impact plane of the armrest foam to 1) the rear of the honeycomb backing plate and 2) the front of the honeycomb. (Figure C7)

- When testing with the CRABI 12, apply contact foil to the door in a space where head contact may occur for either forward facing or rear facing CRS.

- Apply test information placards to the fixture viewable from each camera position.

- Attach the honeycomb to the honeycomb support structure using duct tape.

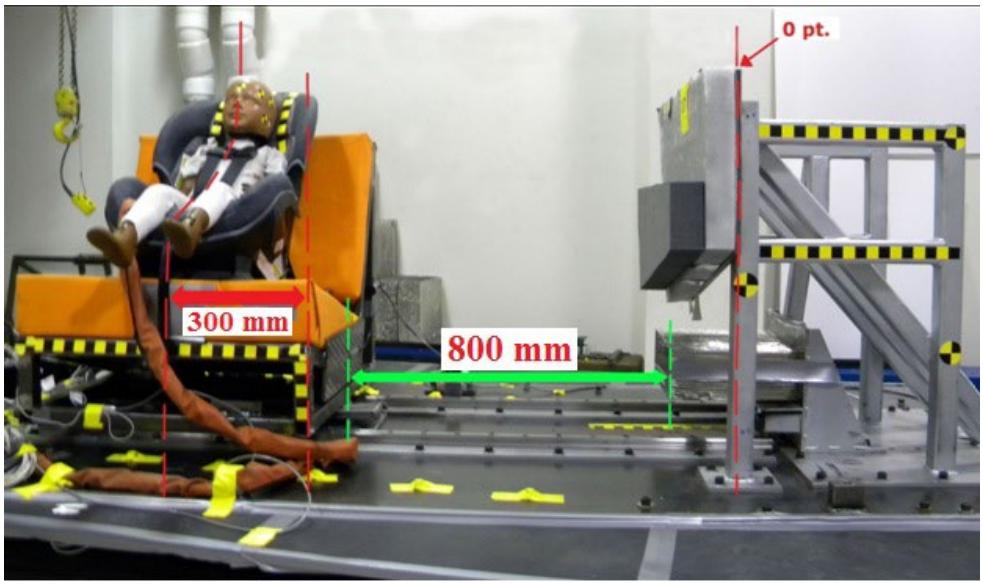

Figure C6: Pretest fixture dimensions

Table C4: Restraint system belt loads

Restraint	Target Load (lbs)
Internal Harness	2.0 to 4.0
Lower Latch Anchors	12.0 to 15.0
Upper Tether	10.0 to 12.0

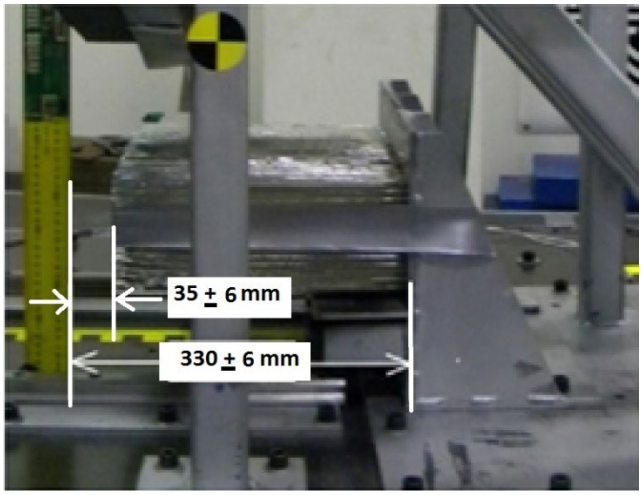

Figure C7: Pretest door surface to honeycomb support surface dimension based on drawing Impactor Frame and Stop Assembly (2921-200) and door foam thickness specifications

Coordinate Measurement Machine (CMM) Pre Test Measurements

Use a CMM such as a FARO arm to measure and record the measurements of the pre-test CRS, test fixture, and ATD positions. Table C5 lists the desired measurement positions for each part. Sample measurements are shown in Table C6. The reference point (or origin) is the upper right corner of the door plate. CMM measurement locations are depicted in Figure C8. Measurement locations will vary for different ATDs and CRS. The Y-axis measurement positions are critical measurements to replicate. Accurate replication of the Y-axis measurements ensures that the CRS is aligned properly on the seat and the dummy is aligned properly in the CRS.

Table C5: CMM measurements

Part	Measurement Position
Fixture	Secondary sled seat forward corner
Fixture	Top forward corner of honeycomb
CRS	Top of seat
CRS	Center of seat base
CRS	Side of base
CRS	Side of CRS
CRS	Center of chest clip
CRS	Center of buckle
ATD	Top of head
ATD	Left head CG
ATD	Front of face
ATD	Left elbow (forward facing)/Right elbow (rear facing)
ATD	Top centerline of right knee
ATD	Top centerline of left knee

Table C6: Sample CMM measurements

Position	Index*	X (mm)	Y (mm)	Z (mm)
Seat base front centerline	1	-181.15	1197.82	414.55
Side of base	2	-445.93	1066.05	447.47
Side of seat	3	-458.33	1027.52	348.82
Top of seat	4	-853.57	1197.02	-54.54
Top of head	5	-702.35	1196.21	-95.54
Front of face	6	-593.29	1199.85	-38.06
Chest clip	7	-538.02	1195.01	80.29
Buckle	8	-404.06	1198.69	224.52
Left knee top	9	-279.20	1111.80	207.78
Right knee top	10	-272.85	1285.07	202.62
Left head CG	11	-680.10	1128.97	-17.91
Elbow	12	-527.11	1078.83	167.25
Sliding seat corner	13	-159.29	893.84	579.76
Honeycomb corner	14	-322.07	82.44	605.09

* Index numbers correspond to Figure C8

Figure C8: Layout of sample CMM measurement locations

Still Photographs

Pre and post test still photographs are taken per the list in Table C7. Placard information labels should be visible in all still photographs. Placard information includes test number, child seat manufacturer and model, CRS attachment method, ATD type, and ATD position. "Pre" or "Post" test label should also be visible.

Table C7: Still photography locations pre and post test

Photo Location / Description	Pre	Post
Front overall	X	X
Front close-up of the ATD in the CRS	X	X
Left	X	X
Left oblique	X	X
Right	X	X
Right oblique	X	X
Rear	X	X
Overhead of sled buck with the CRS and placard in view	X	X
Close-up photo of CRS to document where all targets are on the CRS	X	
Manufacturer label(s)	X	
Overhead view of close-up of impact plane		X
Test photo of chalk marks on seat and door		X
Honeycomb crush with measurement		X
Any damage on CRS (with or without fabric cover)		X
Any damage to test fixture		X

Appendix D: Calculation of Relative Velocity from Deceleration Sled Data

1. Determining the speed at which the primary sled impacts the decelerator

Utilizing the unfiltered, offset acceleration data for the primary sled:

a) Filter primary sled acceleration data using CFC180
b) Integrate the primary sled acceleration with respect to time, setting the final velocity equal to 0.0 at the time which the primary sled has stopped forward motion and prior to the secondary sled impacting the primary sled
c) Determine from the primary sled velocity plot created in Step 1b, the speed at which the primary sled contacts the decelerator. The point-in-time is defined as "time zero" and is defined by a trigger switch between the primary sled and the decelerator. (Figure D1)

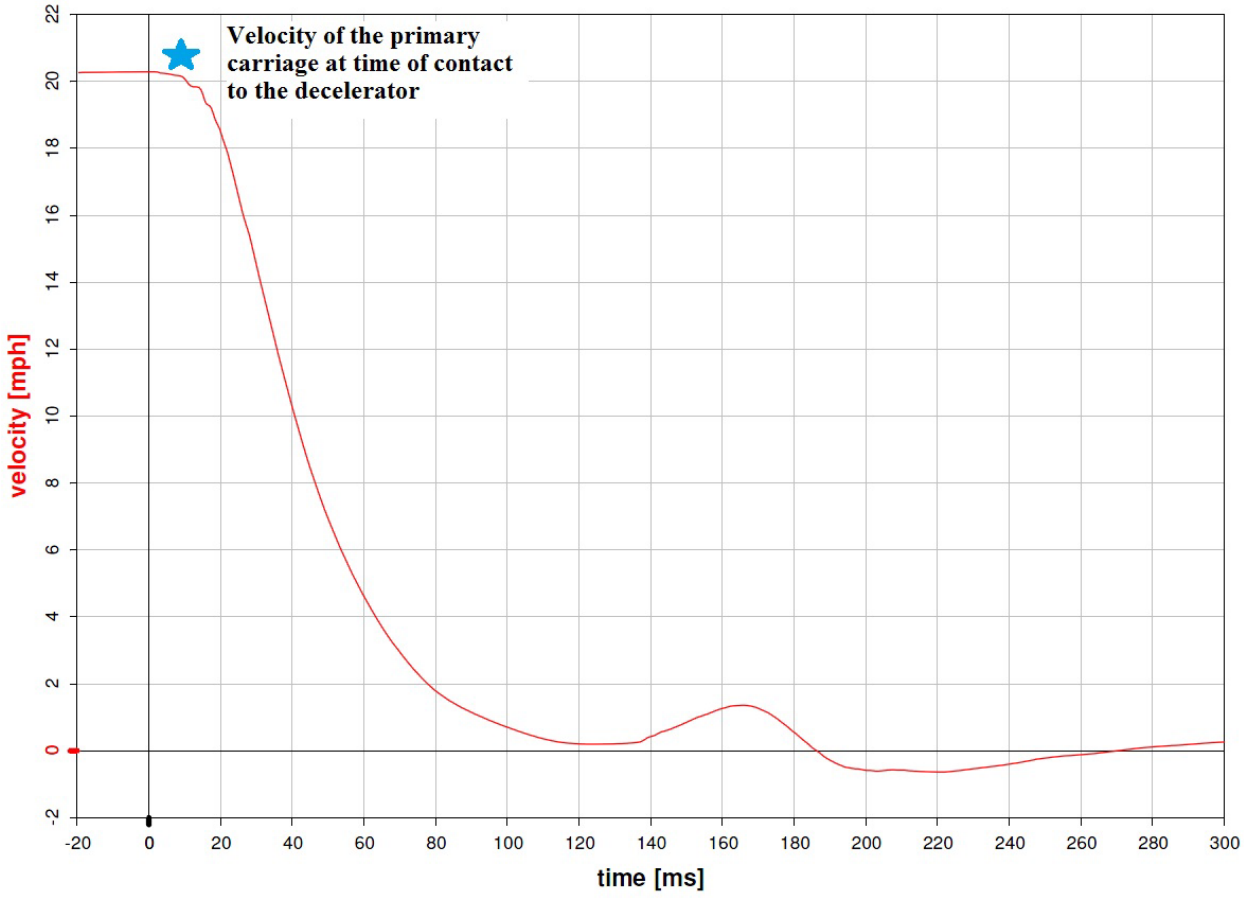

Figure D1: Integration of the primary sled acceleration

2. Determining the speed at which the secondary sled impacts the primary sled

a) The speed determined for the primary sled is the same as the speed of the secondary sled along the longitudinal primary sled axis at "time zero" (as defined as the contact of the primary sled with the decelerator). To determine the speed of the secondary sled along the 10 degree track at "time zero", multiply the primary sled speed (determined in Step 1c) by the cos10 (which equals 0.9848)

Utilizing the unfiltered, offset acceleration data for the secondary sled:

b) Filter secondary sled acceleration data using CFC180
c) Integrate the acceleration of the secondary sled with respect to time, setting the secondary sled speed at "time zero" to the value calculated in Step 2a (Primary Sled Speed * cos 10)
d) Determine from the velocity plot created in Step 2c, the speed at which the secondary sled impacts the aluminum honeycomb. The point-in-time is defined by the trigger switch between the aluminum honeycomb impact plate and the aluminum honeycomb. In the absence of a trigger switch, the point-in-time is defined by the inflection point of the deceleration signal. (Figure D2)

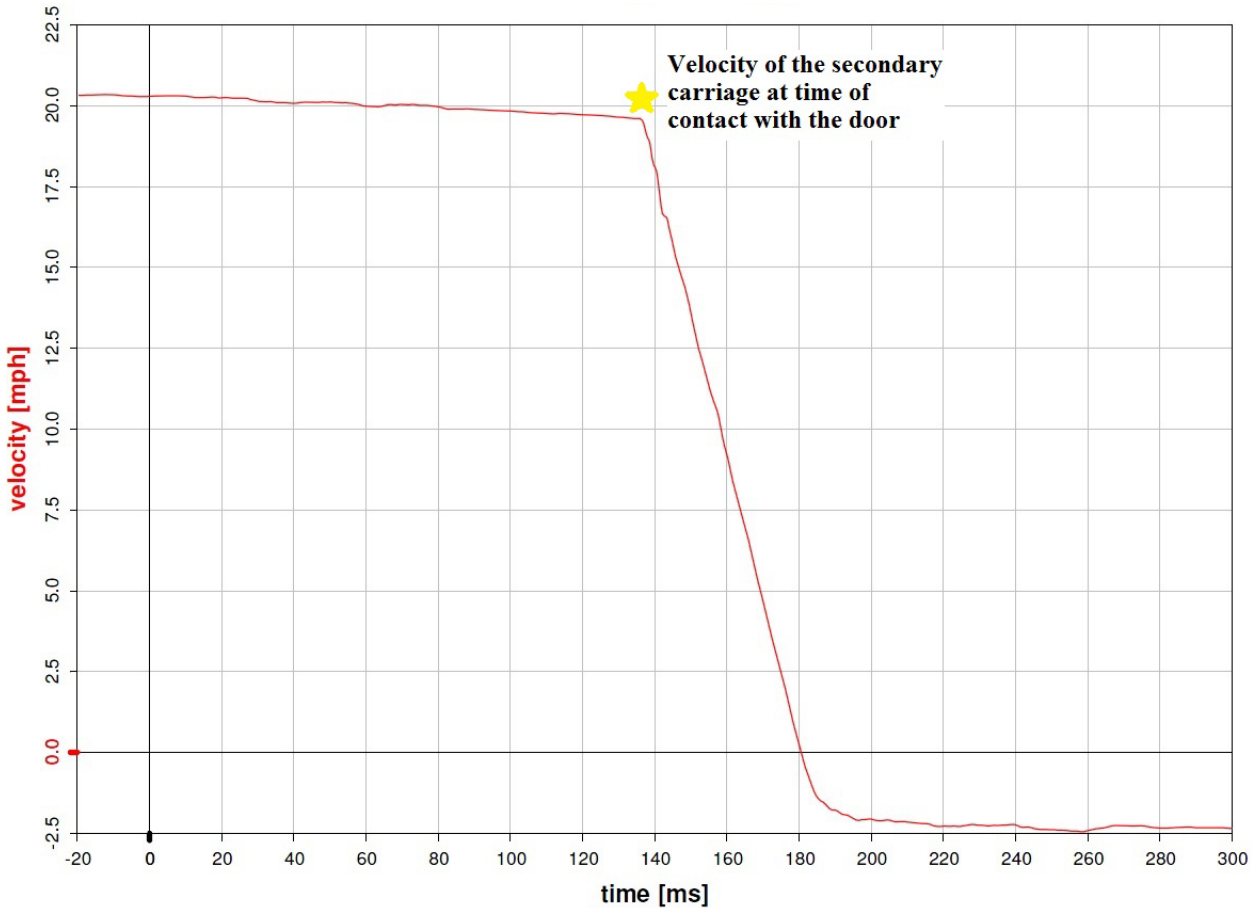

Figure D2: Integration of the secondary sled acceleration

3. Determining the relative velocity

Utilizing the unfiltered, offset acceleration data for the primary and secondary sleds:

a) Filter primary and secondary sled acceleration data using CFC180
b) Subtract the accelerations of the two sleds along the 10 degree track [secondary sled acceleration - (primary sled acceleration * (cos10))]
c) Integrate the difference between the accelerations (data from Section 3b) with respect to time, setting the relative speed at "time zero" to 0.0

d) Determine from the plot calculated in 3c, the speed of the secondary sled at impact with the primary sled, either by use of a trigger switch between the secondary sled aluminum impact plate and the aluminum honeycomb or the inflection point of the relative speed signal. This speed should equate to the speed determined in Section 2d since the primary sled should have reached 0.0 prior to the impact of the secondary sled (Figure D3)

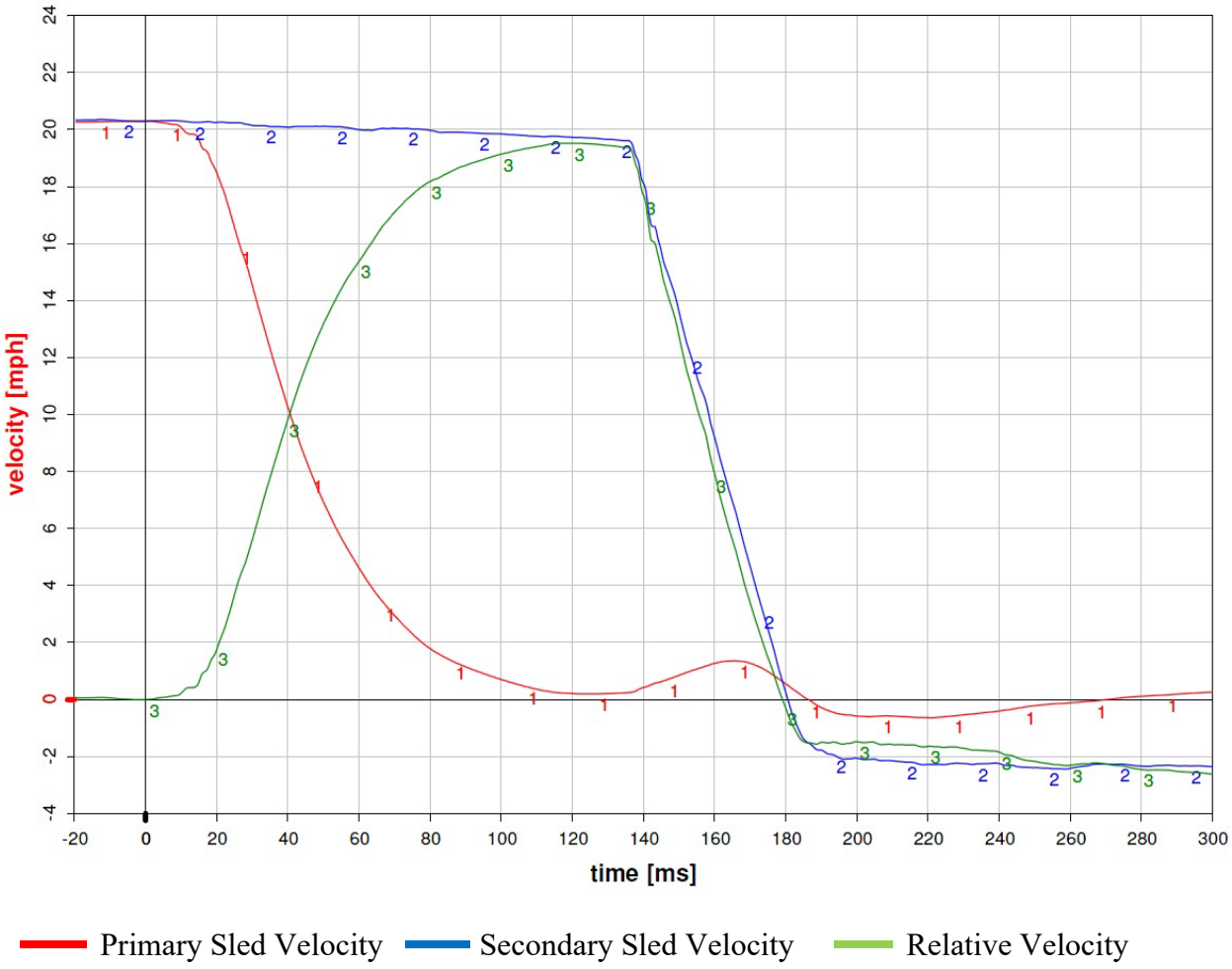

Figure D3: The relative velocity of the secondary sled perpendicular to the door surface and time of contact.

Appendix E: Tabular Data for Tests DOT_SIDE_061 through DOT_SIDE_079

Table E1: Test information and data with fixture speeds and aluminum honeycomb crush

Test Number	ATD	CRS	Orientation	Restraint Type	Primary Sled Overall Velocity [mph]	Secondary Sled Relative Velocity (UPPER) [mph]	Secondary Sled Relative Velocity (MIDDLE) [mph]	Secondary Sled Relative Velocity (LOWER) [mph]	Honeycomb Crush [mm]
SIDE_061	Q3s	Evenflo Maestro	FF	LATCH	20.79	19.49	19.68	19.82	132
SIDE_062	Q3s	Evenflo Maestro	FF	LATCH	20.74	19.57	19.74	19.92	133
SIDE_063	Q3s	Evenflo Maestro	FF	LATCH	21.37	20.27	20.46	20.65	126
SIDE_067	Q3s	Evenflo Maestro	FF	LATCH	20.32	19.40	19.58	19.72	138
SIDE_064	Q3s	Graco Comfort Sport	FF	LATCH	20.72	19.66	19.84	19.91	131
SIDE_065	Q3s	Graco Comfort Sport	FF	LATCH	20.49	19.61	19.73	19.93	132
SIDE_066	Q3s	Graco Comfort Sport	FF	LATCH	20.38	19.52	19.75	20.10	131
SIDE_068	Q3s	Graco Comfort Sport	RF	LA Only	20.34	19.44	19.75	19.84	138
SIDE_069	Q3s	Graco Comfort Sport	RF	LA Only	20.05	19.09	19.25	19.53	140
SIDE_070	Q3s	Graco Comfort Sport	RF	LA Only	20.04	19.11	19.40	19.56	135
SIDE_071	CRABI 12	Chicco KeyFit 30	RF	LA Only	20.29	19.43	19.65	19.91	128
SIDE_072	CRABI 12	Chicco KeyFit 30	RF	LA Only	20.17	19.29	19.46	19.68	132
SIDE_073	CRABI 12	Chicco KeyFit 30	RF	LA Only	20.06	19.10	19.30	19.59	133
SIDE_074	CRABI 12	Britax Boulevard	RF	LA Only	20.08	19.09	19.33	19.64	140
SIDE_075	CRABI 12	Britax Boulevard	RF	LA Only	20.06	19.12	19.27	19.65	142
SIDE_076	CRABI 12	Britax Boulevard	RF	LA Only	20.12	18.99	19.14	19.41	145
SIDE_077	CRABI 12	Cosco Apt 40RF	FF	LATCH	20.06	18.92	19.14	19.48	145
SIDE_078	Q3s	Diono Olympia	RF	LA Only	20.18	19.08	19.44	19.87	143
SIDE_079	Q3s	Diono Olympia	RF	LA Only	19.92	18.45	18.81	19.36	144

Table E2: Q3s test data

Test Number	ATD and Orientation	Head Accel X [g]	Head Accel Y [g]	Head Accel Z [g]	HIC 15 [g]	Upper Spine Y [g]	Pelvis Accel Y [g]	Chest Defl [mm]	Shoulder Disp [mm]	Tether Load [N]
SIDE_061	Q3s - FF	7.06	116.00	16.54	917	92.28	96.42	-23.32	18.91	175.3
SIDE_062	Q3s - FF	7.74	120.20	17.97	963	102.40	100.60	-23.33	17.34	171.8
SIDE_063	Q3s - FF	10.98	118.00	18.10	985	106.50	101.80	-24.45	18.56	199.7
SIDE_067	Q3s - FF	8.70	111.90	18.03	882	101.20	94.72	-23.89	17.79	99.8
SIDE_064	Q3s - FF	-7.45	95.16	36.33	693	90.84	113.10	-22.73	19.60	167.6
SIDE_065	Q3s - FF	-7.37	90.08	37.68	664	95.05	109.00	-21.97	19.00	216.1
SIDE_066	Q3s - FF	-10.81	93.88	42.47	683	93.62	103.40	-22.70	18.56	231.6
SIDE_068	Q3s - RF	-21.84	-77.71	33.10	457	-95.45	-87.23	-33.52	-17.01	N/A
SIDE_069	Q3s - RF	-28.19	-72.74	36.92	481	-93.52	-88.04	-26.12	-15.95	N/A
SIDE_070	Q3s - RF	-27.47	-72.63	47.34	483	-102.70	-92.39	-24.80	-16.49	N/A
SIDE_078	Q3s - RF	-17.34	-131.80	24.49	979	-78.54	-135.00	-34.26	-18.99	N/A
SIDE_079	Q3s - RF	-16.19	-128.80	22.35	955	-77.84	-129.90	-27.32	-18.76	N/A

Table E3: CRABI 12 test data

Test Number	ATD and Orientation	Head Accel X [g]	Head Accel Y [g]	Head Accel Z [g]	HIC 15 [g]	Pelvis Accel Y [g]	Chest Accel X [g]	Chest Accel Y [g]	Chest Accel Z [g]	3ms Clip [g]	Tether Load [N]	Head to Door contact?
SIDE_071	CRABI 12 RF	-10.08	-96.05	30.44	573	-133.9	16.11	-75.14	-28.96	70.23	N/A	NO
SIDE_072	CRABI 12 RF	-14.22	-89.71	28.77	526	-148.0	13.82	-75.79	-22.56	65.81	N/A	NO
SIDE_073	CRABI 12 RF	-12.43	-90.25	33.78	572	-134.8	10.01	-74.60	-14.57	66.91	N/A	NO
SIDE_074	CRABI 12 RF	-19.14	-93.26	19.56	670	-146.7	15.44	-88.65	-12.32	78.98	N/A	NO
SIDE_075	CRABI 12 RF	-22.85	-87.82	20.29	598	-178.0	18.61	-80.49	-10.87	75.41	N/A	NO
SIDE_076	CRABI 12 RF	-23.73	-91.77	14.63	635	-175.2	22.71	-82.19	-12.05	78.08	N/A	NO
SIDE_077	CRABI 12 FF	12.47	122.10	38.57	962	133.9	10.77	115.40	-19.03	93.35	216.8	NO

Appendix F: Head Motion Analysis

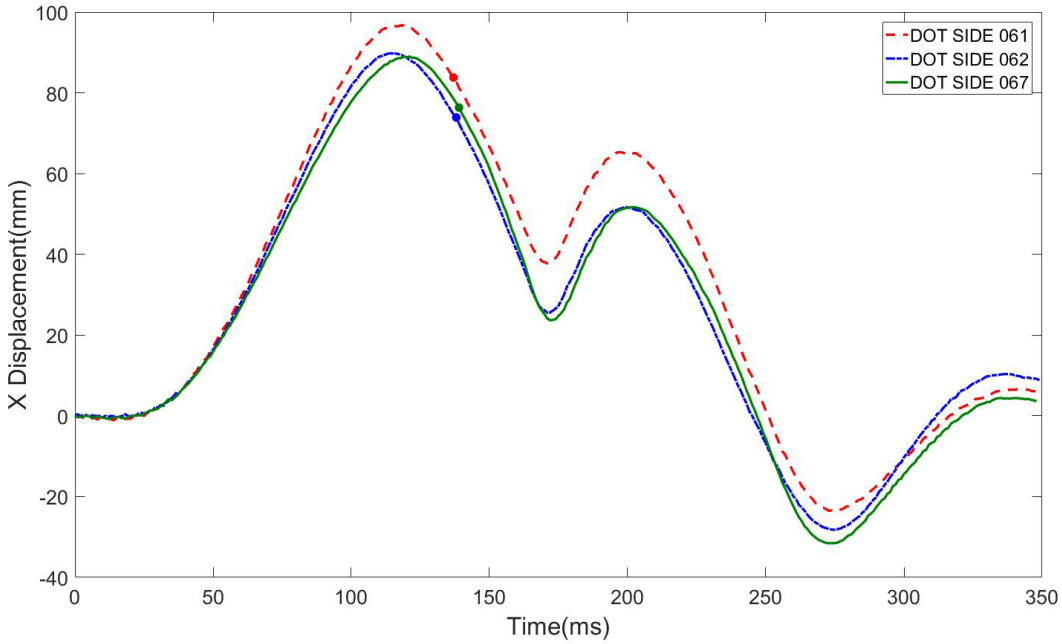

Figure F1: Forward Facing Q3s Evenflo Maestro Head Excursion X-Direction – "•" denotes time of impact of the secondary sled with the aluminum honeycomb

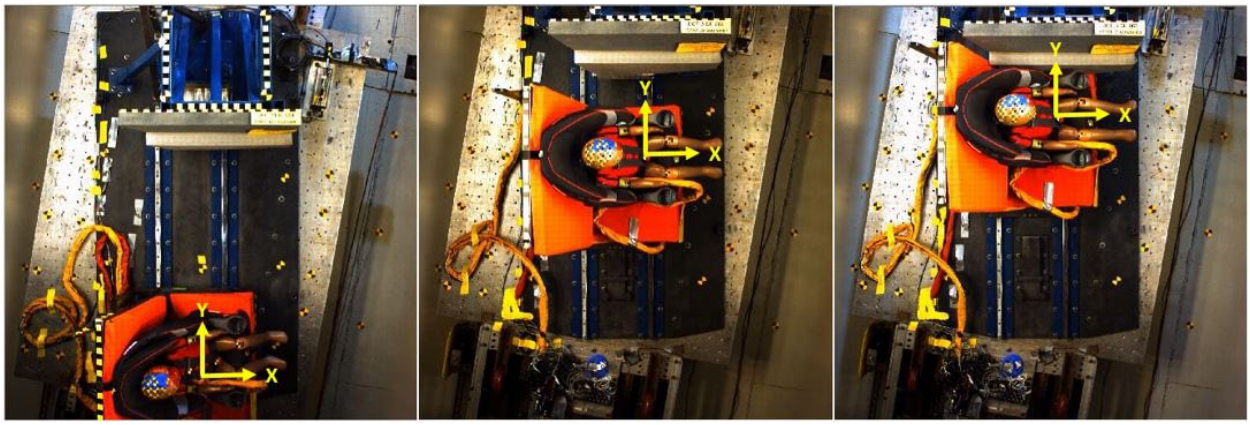

Figure F2: Forward Facing Q3s Evenflo Maestro overhead view at time 0, maximum X-displacement, and secondary impact with the aluminum honeycomb

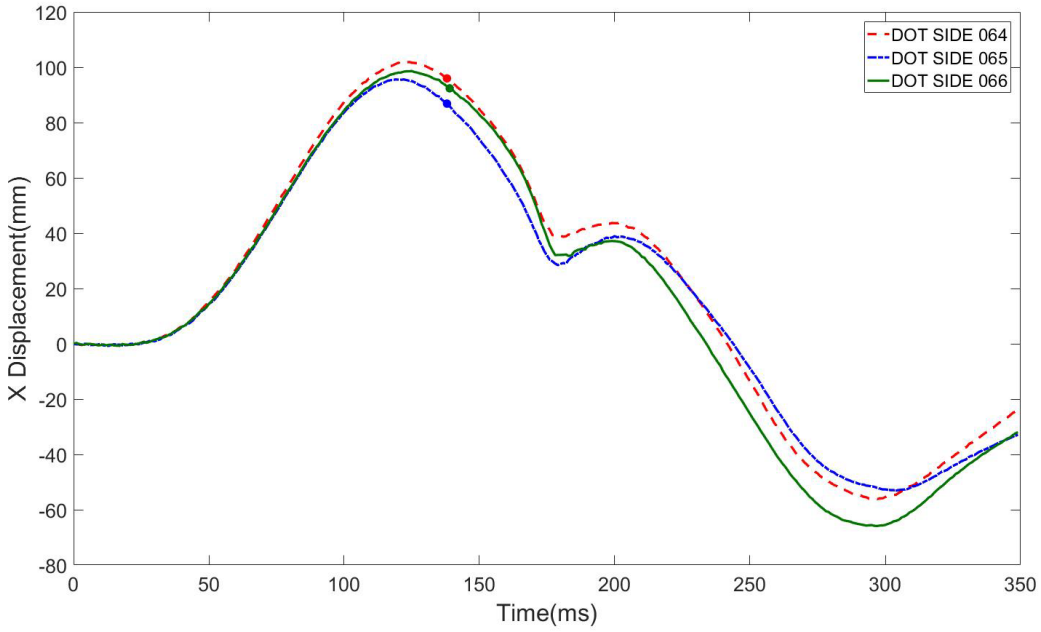

Figure F3: Forward Facing Q3s Graco Comfort Sport Head Excursion X-Direction - "•" denotes time of impact of the secondary sled with the aluminum honeycomb

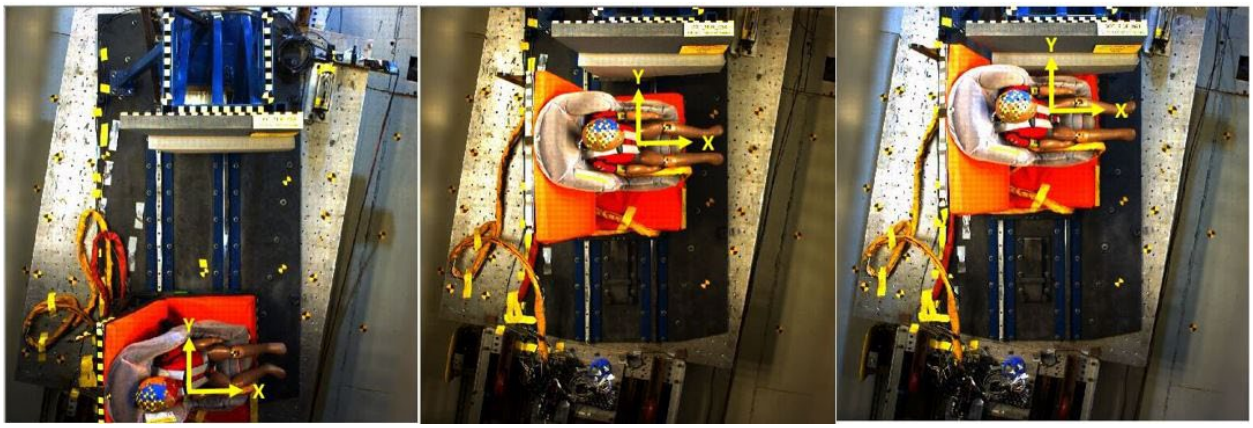

Figure F4: Forward facing Q3s Graco Comfort Sport overhead view at time 0, maximum X-displacement, and secondary impact with the aluminum honeycomb

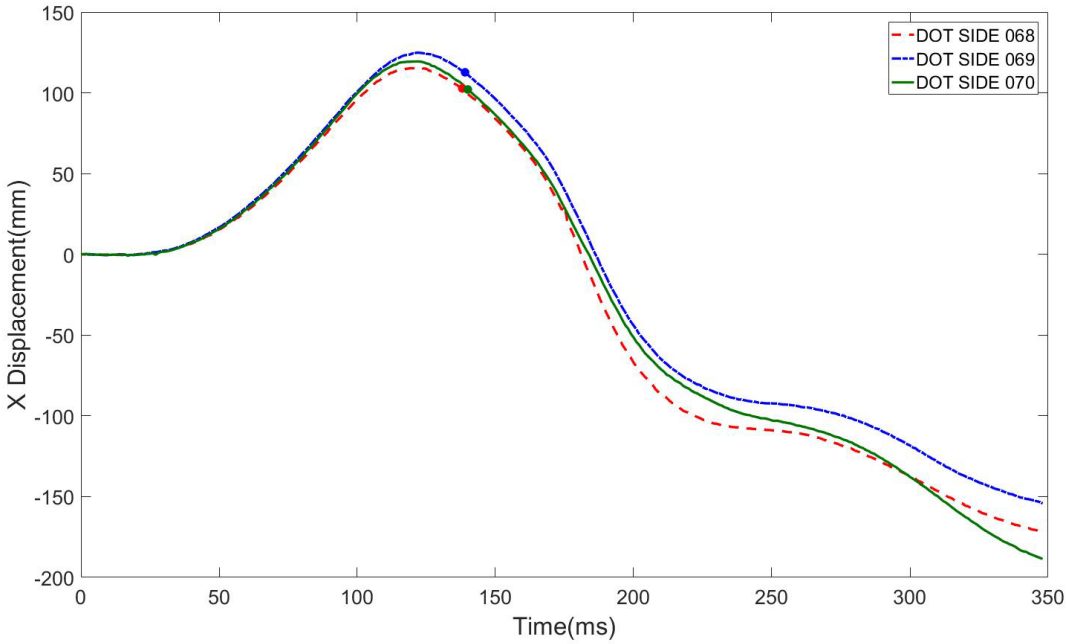

Figure F5: Rear facing Q3s Graco Comfort Sport Head Excursion X-Direction – "•" denotes time of impact of the secondary sled with the aluminum honeycomb

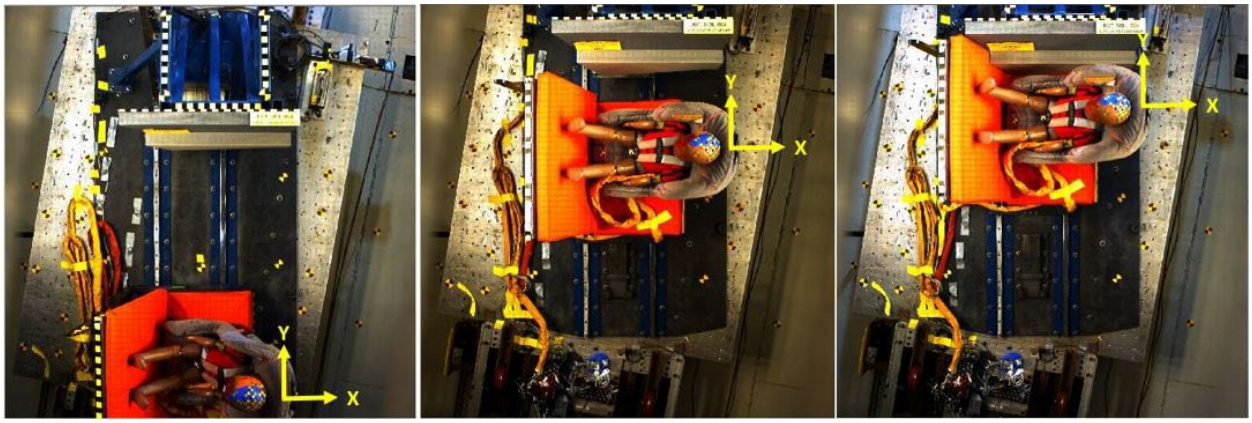

Figure F6: Rear facing Q3s Graco Comfort Sport overhead view at time 0, maximum X-displacement, and secondary impact with the aluminum honeycomb

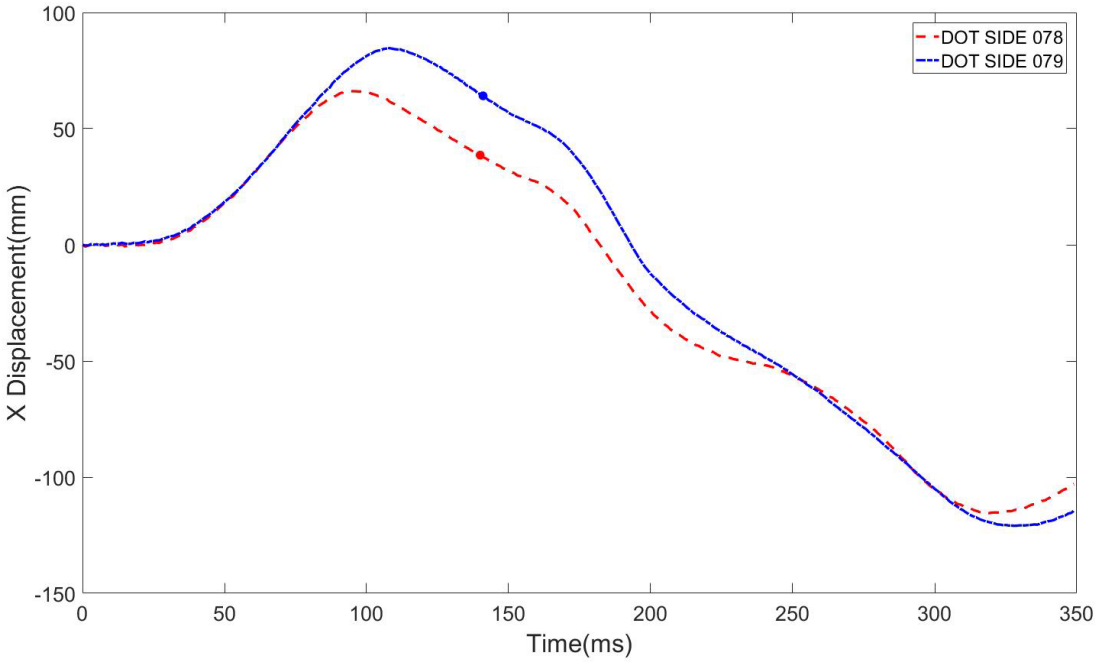

Figure F7: Rear Facing Q3s Diono Olympia Head Excursion X-Direction – "•" denotes time of impact of the secondary sled with the aluminum honeycomb

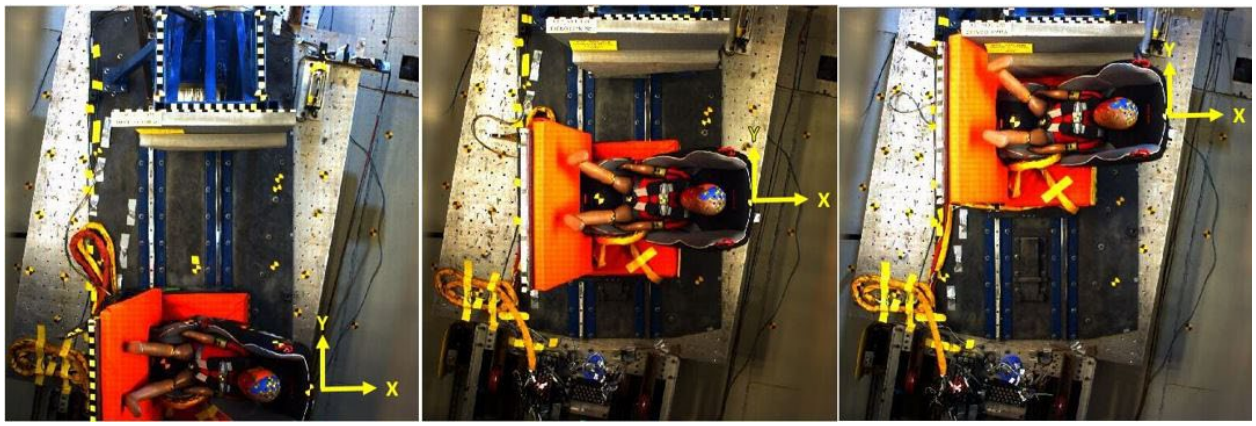

Figure F8: Rear Facing Q3s Diono Olympia overhead view at time 0, maximum X-displacement, and secondary impact with the aluminum honeycomb

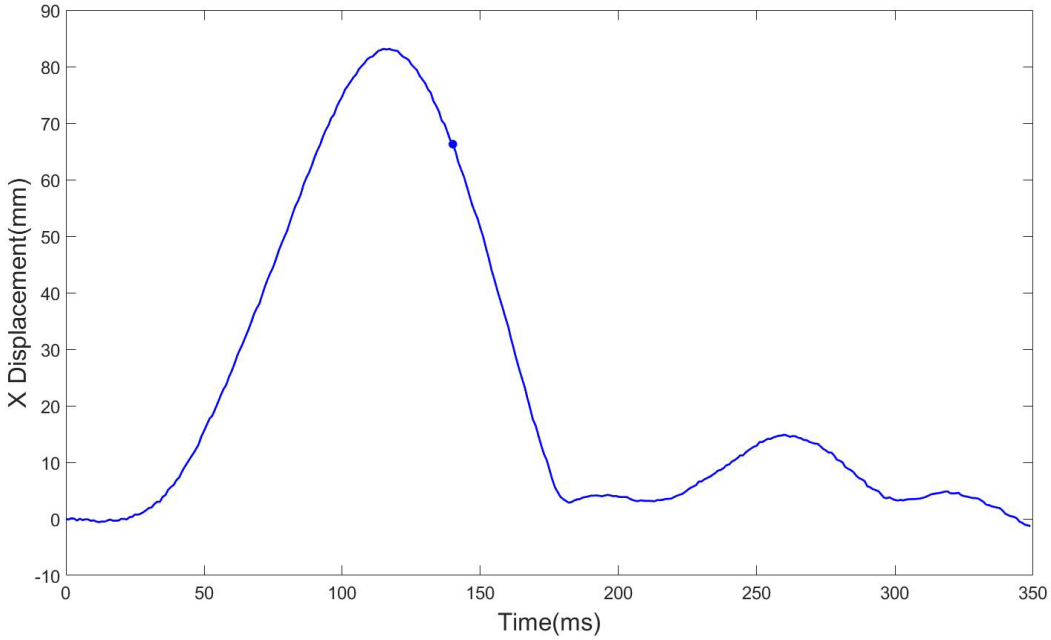

Figure F9 Forward Facing CRABI Cosco APT40RF Head Excursion X-Direction – "•" denotes time of impact of the secondary sled with the aluminum honeycomb

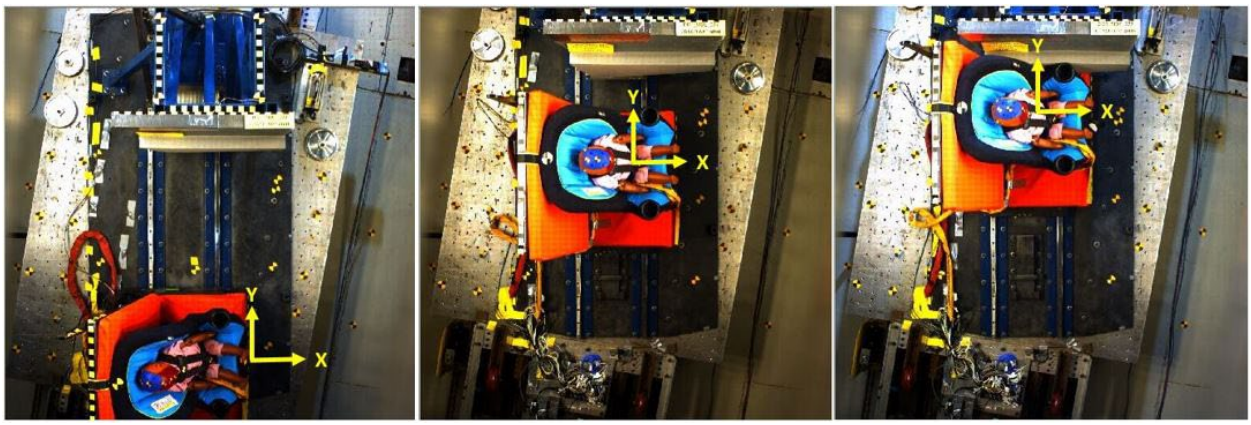

Figure F10 Forward Facing CRABI Cosco APT40RF overhead view at time 0, maximum X-displacement, and secondary impact with the aluminum honeycomb

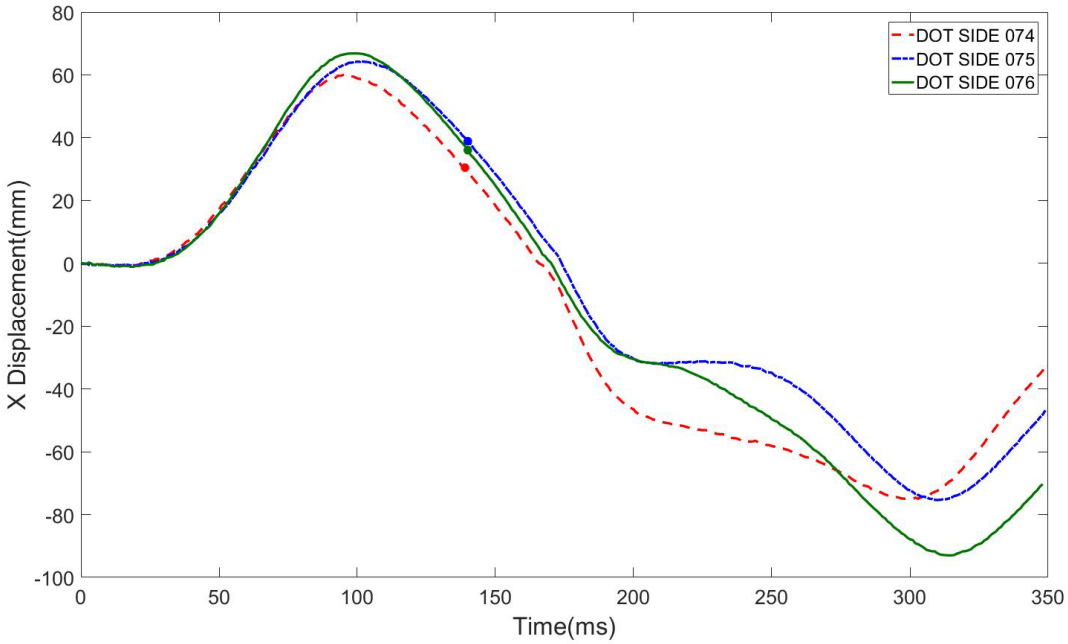

Figure F11: Rear Facing CRABI Britax Boulevard Head Excursion X-Direction – "•" denotes time of impact of the secondary sled with the aluminum honeycomb

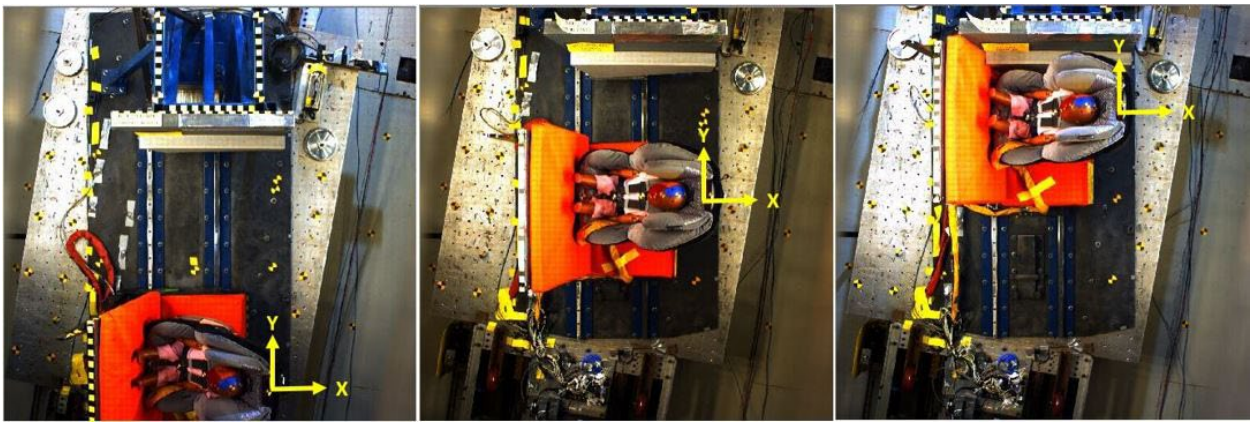

Figure F12: Rear Facing CRABI Britax Boulevard overhead view at time 0, maximum X-displacement, and secondary impact with the aluminum honeycomb

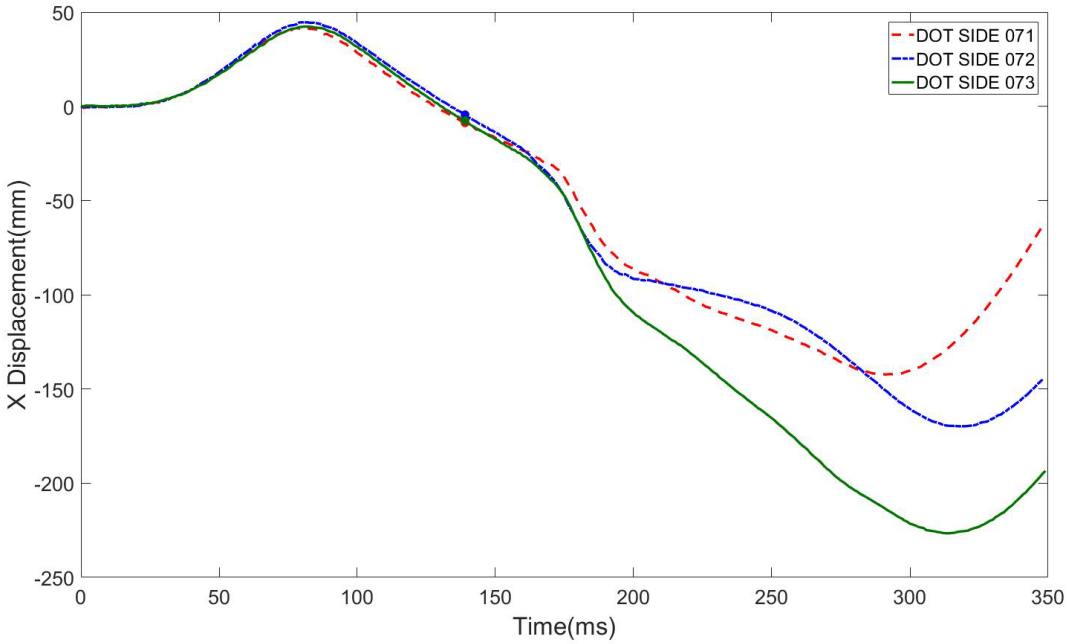

Figure F13: Rear Facing CRABI Chicco Keyfit 30 Head Excursion X-Direction – "•" denotes time of impact of the secondary sled with the aluminum honeycomb

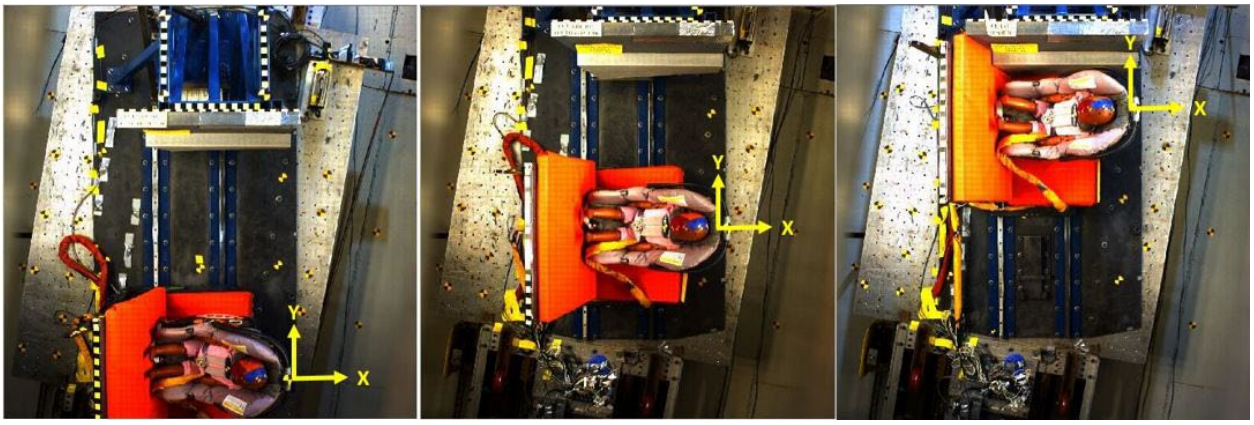

Figure F14: Rear Facing CRABI Chicco Keyfit 30 overhead view at time 0, maximum X-displacement, and secondary impact with the aluminum honeycomb

Table F1: Location of the top of the ATD head at maximum X displacement

Test Number	CRS	Orientation* (FF or RF) and ATD	Time at Max Head Displace-ment (msec)	Top of Head Location X-Direction (mm)	Top of Head Location Y-Direction (mm)
061	Evenflo Maestro	FF Q3s	118	96.7	668.0
062	Evenflo Maestro	FF Q3s	114	89.8	621.7
067	Evenflo Maestro	FF Q3s	121	89.0	685.1
064	Graco Comfort Sport	FF Q3s	124	102.0	723.8
065	Graco Comfort Sport	FF Q3s	122	95.6	695.5
066	Graco Comfort Sport	FF Q3s	125	98.6	720.7
068	Graco Comfort Sport	RF Q3s	119	115.3	680.5
069	Graco Comfort Sport	RF Q3s	122	124.9	701.2
070	Graco Comfort Sport	RF Q3s	122	119.4	699.2
071	Chicco KeyFit 30	RF CRABI 12	81	41.4	329.9
072	Chicco KeyFit 30	RF CRABI 12	82	44.6	344.0
073	Chicco KeyFit 30	RF CRABI 12	82	42.3	333.0
074	Britax Boulevard	RF CRABI 12	95	60.0	448.5
075	Britax Boulevard	RF CRABI 12	102	64.2	499.6
076	Britax Boulevard	RF CRABI 12	100	66.8	494.4
077	Cosco APT40RF	FF CRABI 12	117	83.1	634.1
078	Diono Olympia	RF Q3s	95	66.1	452.0
079	Diono Olympia	RF Q3s	108	84.7	558.6

* Forward Facing (FF) or Rear Facing (RF)

Table F2: Location of the top of the ATD head when the secondary sled impacts the aluminum honeycomb as defined by the trigger switch

Test Number	CRS	Orientation* (FF or RF) and ATD	Time at Secondary Sled Contact (msec)	Top of Head Location X-Direction (mm)	Top of Head Location Y-Direction (mm)
061	Evenflo Maestro	FF Q3s	137	83.8	837.6
062	Evenflo Maestro	FF Q3s	138	73.9	836.6
067	Evenflo Maestro	FF Q3s	139	76.3	844.3
064	Graco Comfort Sport	FF Q3s	138	96.1	849.2
065	Graco Comfort Sport	FF Q3s	138	86.9	837.1
066	Graco Comfort Sport	FF Q3s	139	92.4	845.0
068	Graco Comfort Sport	RF Q3s	138	102.7	851.5
069	Graco Comfort Sport	RF Q3s	139	112.7	854.1
070	Graco Comfort Sport	RF Q3s	140	102.1	860.6
071	Chicco KeyFit 30	RF CRABI 12	139	-8.8	834.7
072	Chicco KeyFit 30	RF CRABI 12	139	-4.5	846.6
073	Chicco KeyFit 30	RF CRABI 12	139	-7.6	828.0
074	Britax Boulevard	RF CRABI 12	139	30.5	835.4
075	Britax Boulevard	RF CRABI 12	140	38.9	830.1
076	Britax Boulevard	RF CRABI 12	140	36.0	844.9
077	Cosco APT40RF	FF CRABI 12	140	66.3	838.4
078	Diono Olympia	RF Q3s	140	38.3	852.3
079	Diono Olympia	RF Q3s	141	64.1	849.8

* Forward Facing (FF) or Rear Facing (RF)